Gain-of-function variants in the ion channel gene *TRPM3* underlie a spectrum of neurodevelopmental disorders

Lydie Burglen[1,2,§], Evelien Van Hoeymissen[3,4,5,§], Leila Qebibo[1], Magalie Barth[6], Newell Belnap[7], Felix Boschann[8], Christel Depienne[9], Katrien De Clercq[3,4,5], Andrew G. L. Douglas[10], Mark P. Fitzgerald[11], Nicola Foulds[12], Catherine Garel[1,13], Ingo Helbig[11], Katharina Held[3,4,5], Denise Horn[8], Annelies Janssens[3,4], Angela M. Kaindl[14-16], Vinodh Narayanan[7], Christina Prager[14,15], Mailys Rupin-Mas[23], Alexandra Afenjar[1], Siyuan Zhao[17], Vincent Th Ramaekers[24], Sarah M Ruggiero[11], Simon Thomas[18], Stéphanie Valence[1,19], Lionel Van Maldergem[20, 21], Tibor Rohacs[17], Diana Rodriguez[1,19], David Dyment[22], Thomas Voets[3,4,##] and Joris Vriens[5, ##]

[1] Centre de référence des malformations et maladies congénitales du cervelet, Département de Génétique, APHP. Sorbonne Université, Hôpital Trousseau, Paris, France

[2] Developmental Brain Disorders Laboratory, Imagine Institute, INSERM UMR 1163, Paris, France

[3] Laboratory of Ion Channel Research, Department of cellular and molecular medicine, University of Leuven, Belgium

[4] VIB Center for Brain & Disease Research, Leuven, Belgium

[5] Laboratory of Endometrium, Endometriosis & Reproductive Medicine, Department Development & Regeneration, University of Leuven, Belgium

[6] Department of Genetics, University Hospital of Angers, Angers, France

[7] Translational Genomics Research Institute (TGen), Neurogenomics Division, Center for Rare Childhood Disorders (C4RCD), Phoenix, Arizona, USA

[8] Charité – Universitäts medizin Berlin, corporate member of Freie Universität Berlin and Humboldt-Universität zu Berlin, Institute of Medical Genetics and Human Genetics, Berlin, Germany

[9] Institute of Human Genetics, University Hospital Essen, University Duisburg-Essen, Essen, Germany

[10] University hospital Southampton nhs foundation trust, UK

[11] Children's Hospital of Philadelphia, Philadelphia, USA

[12] Wessex Clinical Genetics Service, University Hospital Southampton NHS Foundation Trust, Southampton, UK

[13] Service de Radiologie Pédiatrique, Hôpital Armand-Trousseau, Médecine Sorbonne Université, AP-HP, France

[14] Charité – Universitäts medizin Berlin, Department of Pediatric Neurology, Berlin, Germany

[15] Charité – Universitäts medizin Berlin, Center for Chronically Sick Children, Berlin, Germany

[16] Charité – Universitäts medizin Berlin, Institute of Cell Biology and Neurobiology, Berlin, Germany

[17] Department of Pharmacology, Physiology and Neuroscience at Rutgers, New Jersey Medical School, Newark, NJ, USA

[18] Wessex Regional Genetics Laboratory, Salisbury District Hospital, Salisbury, SP2 BBJ, UK

[19] Sorbonne Université, Service de Neuropédiatrie, Hôpital Trousseau AP-HP, SU, F-75012, Paris, France

[20] Centre de Génétique Humaine Université de Franche-Comté Besançon, France

[21] Center of Clinical investigation 1431, National Institute of Health and Medical Research (INSERM), CHU, Besancon, France

[22] Children's Hospital of Eastern Ontario Research Institute, Ottawa, Canada

[23] Department of Neuropediatrics, University Hospital of Angers, Angers, France

[24] Division Neuropediatrics, University Hospital Liège, Liège, Belgium

[§] Shared first authorship

[##] Shared last and corresponding authors

Corresponding authors:

Prof. Joris Vriens

Laboratory of Endometrium, Endometriosis and Reproductive Medicine

Department of Development and Regeneration, KU Leuven

Herestraat 49 box 611, 3000 Leuven, Belgium

Phone:+32 16 327279

Email: Joris.Vriens@kuleuven.be

Prof. Thomas Voets

Laboratory of ion channel Research

VIB-KU Leuven Center for Brain and Disease Research and KU Leuven Department of Molecular Medicine

Herestraat 49 box 801, 3000 Leuven, Belgium

Phone:+32 16 330217

Email: Thomas.Voets@kuleuven. be

ABSTRACT

TRPM3 is a temperature- and neurosteroid-sensitive plasma membrane cation channel expressed in a variety of neuronal and non-neuronal cells. Recently, rare *de novo* variants in *TRPM3* were identified in individuals with developmental and epileptic encephalopathy (DEE), but the link between TRPM3 activity and neuronal disease remains poorly understood. We previously reported that two disease-associated variants in TRPM3 lead to a gain of channel function (Van Hoeymissen et al., 2020; Zhao et al., 2020). Here, we report a further ten patients carrying one of seven additional heterozygous *TRPM3* missense variants. These patients present with a broad spectrum of neurodevelopmental symptoms, including global developmental delay, intellectual disability, epilepsy, musculo-skeletal anomalies, and altered pain perception. We describe a cerebellar phenotype with ataxia or severe hypotonia, nystagmus, and cerebellar atrophy in more than half of the patients. All disease-associated variants exhibited a robust gain-of-function phenotype, characterized by increased basal activity leading to cellular calcium overload and by enhanced responses to the neurosteroid ligand pregnenolone sulphate, when co-expressed with wild-type TRPM3 in mammalian cells. The antiseizure medication primidone, a known TRPM3 antagonist, reduced the increased basal activity of all mutant channels. These findings establish gain-of-function of TRPM3 as the cause of a spectrum of autosomal dominant neurodevelopmental disorders with frequent cerebellar involvement in humans, and provide support for the evaluation of TRPM3 antagonists as a potential therapy.

Key words: TRPM3, gain-of-function, neurodevelopment, intellectual disability, ataxia, cerebellar atrophy, epilepsy

INTRODUCTION

TRPM3, a member of the transient receptor potential (TRP) superfamily of tetrameric ion channels, is a Ca^{2+}-permeable cation channel activated by increasing temperature and by ligands, including the endogenous neurosteroid pregnenolone sulphate (PS) (1, 2). The channel is best known for its role in peripheral somatosensory neurons, where it is involved in heat sensation and in the development of pathological pain (1, 3, 4). In addition, TRPM3 is expressed in kidney, eye, pancreas, and several regions of the central nervous system, such as the hippocampal formation, the choroid plexus and the cerebellum, but little is known about the channel's physiological role in these brain tissues (5-7).

Rare *de novo* nonsynonymous coding variants in neuronally expressed genes are frequent causes of global developmental delay (GDD) and intellectual disability (ID) (8). Recently, *de novo* variants in *TRPM3* were reported in patients with developmental and epileptic encephalopathy, including 16 patients with the recurrent missense variant p.Val1002Met, and two additional patients with the variants p.Pro1102Gln and p.Ser1367Thr, respectively (9-13) (see results and Figure 1 for further discussion and details on numbering of *TRPM3* variants). These patients consistently present with moderate-to-severe GDD and ID, variably associated with other clinical features such as childhood-onset epilepsy, hypotonia, altered heat and/or pain sensitivity and variable facial dysmorphism. Functional characterization of the p.Val1002Met and p.Pro1102Gln variants in heterologous expression systems indicated that both lead to a gain of channel function (14, 15). However, the relation between TRPM3 channel function and neuronal disease remains poorly understood, and it is unknown whether other variants in *TRPM3* can cause human disease.

Here, we report the clinical characteristics of ten individuals exhibiting one of seven previously unreported heterozygous missense variants, and highlight a novel cerebellar phenotype observed in more than half of the patients. Functional characterization of the newly discovered *TRPM3* missense variants in a human cell line revealed a consistent and robust increase in channel activity when co-expressed with wild-type TRPM3 subunits. These findings establish gain-of-function variants in *TRPM3* as pathogenic, causing an autosomal dominant neurodevelopmental syndrome with frequent cerebellar involvement.

118 # RESULTS

119 **Organization of the human *TRPM3* gene and alternative splicing in the cerebellum**

120 The *TRPM3* primary transcript can undergo alternative splicing at multiple sites, leading to a
121 large number of potential splice variants that encode gene products of different lengths.
122 More specifically, there are two alternative, mutually exclusive first exons (exon 1 and exon
123 2), potential exon skipping at exons 8, 15, and 17, an alternative 5' splice site in exon 24, and
124 intron retention in the final exon 28 (Figure 1A). Recent studies indicate that alternative
125 splicing can have an important impact on TRPM3 channel functionality: the presence of exon
126 17 is essential for inhibitory regulation of TRPM3 by the $G_{\beta\gamma}$ subunit of trimeric G proteins
127 (16), whereas the use of alternative 5' splice sites in exon 24 leads to channel isoforms with
128 either a short or a long pore loop, exhibiting distinct cation selectivity and sensitivity to the
129 neurosteroid PS (6, 17-19). However, the impact of other splicing events on channel function
130 remains unclear, with several splice variants that can be heterologously expressed as
131 channels with indistinguishable functional properties (15-17). The existence of multiple
132 transcripts has caused ambiguity in the amino acid numbering of channel variants in
133 patients, and the frequency of the different alternative splicing events in disease-relevant
134 tissue is currently unknown.

135 To address this issue, we analyzed a publicly available RNA-seq dataset from human
136 cerebellum and used the Sashimi plot feature of the Integrative Genomics Viewer to quantify
137 the frequency of the different potential alternative splicing events. This analysis indicates
138 that the large majority of transcripts in human cerebellum use exon 2 as first exon (85%),
139 have a short pore loop (>98%), and do not undergo intron retention in exon 28 (82%).
140 Moreover, a variable number of transcripts included the optional exons 8 (12%), 15 (41%)
141 and 17 (85%). A construct using exon 2 as the start exon, with a short pore, including all
142 three optional exons as well as the full exon 28 (transcript variant NM_001366147.2),
143 corresponding to a protein of 1744 amino acids, did, however, not yield a functional channel
144 upon heterologous expression in HEK293T cells (Figure 1 - Figure supplement 1). In contrast,
145 a construct lacking the lowly expressed exon 8 (transcript NM_001366145.2) yielded robust
146 TRPM3-dependent signals upon expression in HEK293T cells, as assessed using Fura-2-based
147 calcium microfluorimetry and whole-cell patch-clamp experiments. This included robust

148 responses to PS stimulation and potentiation by co-application of PS + clotrimazole (20)
149 (Figure 1 - Figure supplement 1). We propose to use the latter transcript as the reference for
150 variant numbering, as it represents the longest functional splice variant that includes all
151 exons that are frequently used in human brain tissue and covers all human disease-
152 associated *TRPM3* variants. For instance, according to this nomenclature, the recurrent
153 variant initially indicated as p.Val837Met (9-11, 21) will be named p.Val1002Met.

154 **Identification of *TRPM3* variants in patients with neurodevelopmental disorders**

155 Through collaborations and research networks, we ascertained ten patients carrying *TRPM3*
156 variants (8 females, 2 males; age 21 months to 45 years). Eight individuals carried a *de novo*
157 variant while one male patient had inherited the variant from his mildly affected father. Like
158 patients harboring the recurrent p.Val1002Met *TRPM3* variant, patients with the novel
159 variants presented with a neurodevelopmental disorder of variable severity, variably
160 associated with skeletal abnormalities and epilepsy. Clinical summaries of the patients are
161 presented in Table 1, summarizing the core phenotypic features of the ten patients. The first
162 symptoms were observed within the first year of life in 8 out of 10 patients, and included
163 hypotonia, poor visual contact or pursuit and motor delay. In one patient, the first concern
164 was an unstable, ataxic standing at 14 months. One patient showed a slight motor delay in
165 childhood and had mild intellectual deficiency but was only diagnosed when his son was
166 investigated for the same condition. Gross motor milestones were delayed in 9 out of 10
167 patients, autonomous walking was achieved late, between 19 and 25 months in 4 out of 10
168 patients, walking with aid in one patient at 4 years, and walking was not achieved in 4 out of
169 10 patients (ages 21 months - 3 years - 10 years - 20 years at time of study). Patients were
170 stable or made developmental progress, but one individual had several episodes of
171 behavioral changes with irritability, which were associated with transient degradation in
172 motor skills. Four patients had cerebellar ataxia, and two other patients showed severe
173 hypotonia without weakness and with nystagmus, that may be related to cerebellar
174 involvement. Language development was normal in 3 out of 10 patients, delayed in 3
175 patients, and absent in 4 patients. Two of the latter are able to communicate using non-
176 verbal tools like pictograms. Intellectual deficiency (ID) was observed in all subjects, ranging
177 from a low normal-mildly reduced IQ in 3 out of 10 patients to severe intellectual deficiency
178 in 4 patients. There were no striking behavioral anomalies, except for patient n° 5 who

179 displayed food-seeking behavior responsible for his obesity. One patient had febrile seizures.
180 Epilepsy was diagnosed in only 2 patients: one patient had nocturnal generalized tonic-clonic
181 seizures since 7 years of age, and a further patient had electrical status epilepticus during
182 slow-wave sleep (ESES). Moreover, in a third patient, epilepsy was doubtful and an epileptic
183 therapy was started (patient n° 4). Note that sleep electroencephalograms (EEGs) were not
184 performed in all patients. None was refractory to anti-seizure medication. None of the
185 patients had hearing loss and there was not a clearly recognizable facial dysmorphism.
186 Notably, 7 out of 10 patients showed skeletal anomalies: hip subluxation (2), patellar
187 dislocation (1), Perthes' disease (1), brachydactyly (1), valgus foot (2), and rib hypoplasia (1).
188 Two patients had a statural growth restriction and 3 out of 10 patients showed mild
189 proportional secondary microcephaly. Cranial Magnetic Resonance Imaging (MRI) was
190 normal in 3 out of 8 patients. However, a substantial number of patients showed cerebellar
191 atrophy (5 out of 8 patients): vermian and cerebellar hemispheres atrophy in patients n° 1-4
192 (Figure 2 and Table 1), and a localized partial atrophy of both cerebellar hemispheres in
193 patient n° 7 (Figure 2 - Figure supplement 1). Serial cranial MRI performed in three patients
194 showed that the atrophy was progressive, and was not present in MRI performed in the first
195 months of life (Figure 2). Finally, 4 out of 10 patients exhibit pain insensitivity and 2 patients
196 showed heat insensitivity.
197 Genetic analyses identified seven novel *TRPM3* heterozygous variants in a total of ten
198 affected patients (Table 1 and Figure 1). All variants were absent from the gnomAD database
199 and predicted to be pathogenic according to at least 2 out of 4 prediction meta-analysis
200 programs like REVEL (CADD, DANN and PROVEAN) (Table 3) (22). Eight variants occurred *de*
201 *novo* and one was inherited from the affected father. Sequence alignment at position D614,
202 L769, V1002, G1007, P1102, N1126 and S1133 shows that the variants are located in highly
203 conserved areas, both across orthologues from multiple species (Drosophila, zebrafish,
204 mouse, rat, macaca) and in the most closely related homologues within the TRPM subfamily,
205 namely TRPM1, TRPM6 and TRPM7 (Figure 1 - Figure supplement 3). The previously
206 identified and novel disease-associated variants localize to different regions of TRPM3,
207 including the cytosolic N-terminus (D614V and L769V), the transmembrane region (V1002M,
208 V1002G, V1002L, G1007S and P1102Q) and the cytosolic C-terminus of the channel (N1126D,
209 S1133P and S1392T) (Figure 1 - Figure supplement 3).

210 When mapped on the recent cryo-EM structure of TRPM3 in the closed state and in the
211 presence of $G_{\beta\gamma}$ (pdb:8DDQ) (23), it can be noted that many of the disease-associated
212 variants cluster at the interface between the transmembrane domain and the cytosol (Figure
213 1 - Figure supplement 2). Notably, the N-terminal L769 sits in close proximity to V1002 and
214 G1007 at the cytosolic end of transmembrane helix S4 and the S4-S5 linker, whereas N1126
215 and S1133 are located in the cytosolic TRP helix, which runs parallel to the plasma
216 membrane, in close proximity to the S4-S5 linker. Thus, disease-associated variants affecting
217 these residues are localized in a region that is critically involved in the gating of TRP and
218 related voltage-gated cation channels. Interestingly, residue D614 is located in a cytosolic
219 loop that is disordered in the cryo-EM structures. In the structure of the TRPM3 channel
220 subunit in contact with nanobody-tethered $G_{\beta\gamma}$ (pdb:8DDQ), D614 is located just adjacent to
221 the TRPM3-$G_{\beta\gamma}$ interaction site(16, 23) raising the possibility that charge neutralization in the
222 D614V variant may affect $G_{\beta\gamma}$-dependent channel regulation (Figure 1 - Figure supplement
223 2).

224 **Functional expression of disease-related *TRPM3* variants**

225 To address whether the seven newly identified variants affect TRPM3 channel activity, we
226 introduced the corresponding point mutations into a previously well-characterized human
227 TRPM3 expression vector for heterologous expression (14). Fura-2-based calcium imaging in
228 transfected HEK293T cells was used to evaluate basal channel activity and responses to the
229 TRPM3 antagonist primidone (24) and to investigate the sensitivity towards stimulation via
230 the agonist pregnenolone sulphate (PS). In line with earlier work, cells transfected with the
231 wild-type (WT) TRPM3 construct showed a small increase in basal intracellular calcium
232 concentration ($[Ca^{2+}]_i$) compared to non-transfected (NT) cells. In WT transfected cells, the
233 cytosolic $[Ca^{2+}]_i$ decreased slightly in response to treatment with a high dose of primidone
234 (100 µM) (Figure 3A, B, Figure 3 – Figure Supplement 1 and Figure 4 – Figure supplement 1).
235 The primidone dose was based on earlier work, demonstrating a lower sensitivity of *TRPM3*
236 variants p.Val1002Met and p.Pro1102Gln towards primidone stimulation (14, 15).

237 When overexpressing the newly identified TRPM3 variants, with the exception of the L769V
238 variant, we consistently observed basal $[Ca^{2+}]_i$ levels that were significantly higher compared
239 to NT cells or cells transfected with WT-TRPM3, an effect that was most pronounced for the
240 V1002G variant (Figure 3A, B, Figure 3 – Figure Supplement 1 and Figure 4 – Figure

241 supplement 1). Except for the L769V and the G1007S variant, application of primidone
242 caused a reduction of $[Ca^{2+}]_i$, albeit not to the levels of NT cells (Figure 3A, B, Figure 3 –
243 Figure Supplement 1 and Figure 4 – Figure supplement 1). These results indicate that the
244 patient variants lead to increased basal TRPM3 activity. A more mixed result was obtained
245 when assessing the responses of the variants to the neurosteroid agonist PS. Compared to
246 WT-TRPM3, PS responses were increased for the D614V, N1126D and S1133P variants, and
247 reduced for the L769V, V1002G, V1002L and G1007S variants (Figure 3C, D, Figure 3 – Figure
248 Supplement 2 and Figure 4 – Figure Supplement 2).

249 Note that all described patients are heterozygous for the specific TRPM3 variants, and thus
250 possess one wild-type allele. To mimic the patient situation in our cellular assay, we
251 performed experiments in HEK293T cells transfected with a mixture of cDNA encoding WT
252 and variant TRPM3 in a 1:1 ratio. Under these conditions, significantly higher basal $[Ca^{2+}]_i$
253 levels for all wild-type/variant mixtures were observed compared to cells expressing only
254 WT-TRPM3, with the exception of the P1102Q and N1126D variant, where the elevated
255 basal $[Ca^{2+}]_i$ levels were found not to be significant. Moreover, under these heterozygous
256 conditions, primidone caused a reduction in basal $[Ca^{2+}]_i$ for all tested variants with higher
257 basal $[Ca^{2+}]_i$ levels (Figure 4A, B, Figure 3 – Figure Supplement 1 and Figure 4 – Figure
258 Supplement 1). Finally, cells co-expressing WT-TRPM3 with any of the newly discovered
259 disease-associated variants consistently exhibited larger PS-induced Ca^{2+} responses (Figure
260 4C, D, Figure 3 – Figure Supplement 2 and Figure 4 – Figure Supplement 2).

261 Since the calcium imaging experiments suggested that the L769V and G1007S variants had
262 opposite effects on channel activity when expressed alone versus combined with WT
263 subunits, we further evaluated their functionality using whole-cell patch-clamp
264 electrophysiology. We measured whole-cell TRPM3 currents in response to a voltage step
265 protocol ranging from -160 mV to +160 mV (Figure 4 – Figure Supplement 3), both at
266 baseline and upon stimulation with PS. At room temperature, and in the absence of
267 activating ligand, WT-TRPM3 carries a small, outwardly rectifying current (1, 2). We observed
268 that cells expressing WT+L769V, G1007S and WT+G1007S produced robust outwardly
269 rectifying currents, whereas currents in cells expressing only L769V were not different from
270 those in non-transfected (NT) cells (Figure 4 – Figure Supplement 3B). Upon stimulation with
271 PS, robust outwardly rectifying currents were evoked in cells expressing WT, WT+L769V,

272 G1007S and WT+G1007S, whereas currents in cells expressing L769V were not different from
273 those in non-transfected controls (Figure 4 – Figure Supplement 3D). Notably, in cells
274 expressing WT+L769V, we measured an increase in inward current at -160 mV when
275 compared to non-transfected controls, reminiscent of the inwardly rectifying current
276 component observed in the V1002M variant (Figure 4 – Figure Supplement 3E) (14).

277 Since the G1007S variant showed a reduced Ca^{2+} response to PS stimulation in the
278 homozygous condition, but a significantly increased PS response in the heterozygous
279 condition, we tested the concentration dependence of the response to PS for this variant
280 using a calcium-based assay performed in a plate-reader system. These experiments
281 revealed a shift of the concentration-response curve to lower PS concentrations for the
282 heterozygous, but not for the homozygous condition (EC_{50} value of 2.9 ± 0.3 µM, 4.0 ± 0.5
283 µM and 1.1 ± 0.1 µM for respectively WT-TRPM3, homozygous G1007S and heterozygous
284 WT+G1007S transfected HEK293 cells) (Figure 3 – Figure Supplement 3). Taken together,
285 these data demonstrate that all patient variants are dominant gain-of-function mutations,
286 provoking significantly increased basal activity resulting in cellular calcium overload, as well
287 as enhanced PS-induced responses.

288 To investigate whether alterations in the cellular expression levels of the variant TRPM3
289 channel subunits contribute to the increased channel activity, we measured single-cell YFP
290 fluorescence and basal $[Ca^{2+}]_i$ levels in HEK293T cells transfected with the different TRPM3
291 variants (either alone or in combination with WT-TRPM3), and compared them with levels in
292 cells transfected with WT-TRPM3 on the same experimental day. For variants V1002L,
293 G1007S, N1126D and S1133P, YFP levels were not higher than in cells expressing WT-TRPM3,
294 similar to our earlier observations for the V1002M and P1102Q variants (14) (Figure 3 –
295 Figure Supplement 4). In cells expressing the L769V variant in the absence of WT subunits,
296 which do not show a response to the channel antagonist primidone or the channel agonist
297 PS (Figure 3), cellular YFP values were significantly reduced compared to WT (Figure 3 –
298 Figure Supplement 4). However, normal YFP levels were found in cells co-expressing the
299 L769V variant with WT (Figure 3 – Figure Supplement 4). Finally, in the case of D614V and
300 V1002G variants, cellular YFP levels were significantly higher than WT control, both under
301 homozygous and heterozygous conditions (Figure 3 – Figure Supplement 4). To evaluate
302 whether the increased basal activity for these variants is a mere consequence of the

303 increased channel expression levels, we plotted basal $[Ca^{2+}]_i$ versus cellular YFP levels for
304 individual cells expressing either WT, variant or WT + variant. This analysis revealed that, in
305 cells with similar YFP fluorescence, basal $[Ca^{2+}]_i$ levels were consistently higher for cells
306 expressing the D614V and V1002G variants, either alone or with WT subunits (Figure 3 –
307 Figure Supplement 4).

308 Taken together, these data indicate that elevated basal $[Ca^{2+}]_i$ levels in cells expressing
309 disease-associated TRPM3 variants can be attributed to increased activity of individual
310 channels rather than to increased channel protein expression.

311 **DISCUSSION**

312 TRPM3 is a calcium-permeable cation channel belonging to the melastatin subfamily of
313 transient receptor potential channels. It functions as a heat- and neurosteroid-activated
314 channel in peripheral sensory neurons of the trigeminal and dorsal root ganglia (4), but is
315 also expressed in other tissues, including the central nervous system (Figure 5 – Figure
316 supplement 1). Recently, three *de novo* variants in the *TRPM3* gene were identified in
317 patients with developmental and epileptic encephalopathies (DEE) (9-13). The 16 patients
318 heterozygous for the common recurrent variant (V1002M), share a number of clinical
319 features including global developmental delay (GDD), moderate to severe intellectual
320 disability (ID), with or without childhood-onset epilepsy (13).
321 Here, we describe patients carrying one of seven novel *de novo* variants in the *TRPM3* gene.
322 These patients present with a large spectrum of neurodevelopmental symptoms, including
323 global developmental delay and intellectual disability, variably associated with seizures,
324 skeletal anomalies and insensitivity to pain and heat. Intellectual deficiency as well as motor
325 disabilities are highly variable, from polyhandicap to very mild impact compatible with
326 parentality and normal life in adulthood. We highlight a cerebellar phenotype (ataxia or
327 severe hypotonia, nystagmus or abnormal oculomotricity, cerebellar atrophy) in more than
328 half of the patients as a novel feature of the TRPM3-linked disease pattern. The cerebellum
329 is known to integrate neuronal networks coupling motor function with cognition, emotional
330 skills and language (25-27). Distortion of cerebellar development could induce (cerebellar)
331 diseases (26). Abundant RNA expression of TRPM3 in the brain are already described (19),
332 however, limited knowledge is available on the functional expression of TRPM3 in the
333 central nervous system, including cerebellar Purkinje cells and oligodendrocytes (7, 19, 28,
334 29). By reanalyzing publicly available single cell RNA sequencing datasets of the developing
335 (30) and adult (31) cerebellum and adult cortex (32), it becomes apparent that TRPM3 is
336 robustly expressed in different cell types of these brain regions (Figure 5 and Figure 5 –
337 Figure Supplement 2). Highest expression of TRPM3 in the adult cortex (32) was found in
338 layer 5/6 neurons (Figure 5 – Figure Supplement 2A, C, E). Furthermore, TRPM3 expression
339 was observed in distinct cellular clusters of the adult cerebellum (31), including neuronal
340 (e.g. distinct cerebellar granule cells and Purkinje neurons) and non-neuronal (e.g.
341 cerebellar-specific astrocytes) cell types (Figure 5B, D, F). Interestingly, prominent TRPM3

342 expression was observed in early stages of the developing cerebellum (Figure 5 – Figure
343 Supplement 2B, D) and detected in different cell types (Figure 5A, C, E), including excitatory
344 cerebellar and unipolar brush cell interneurons, and Purkinje cells (30). Highest expression is
345 noted in cells of the rhombic lip (Figure 5A, C, E, G), where TRPM3 is expressed in all four
346 zones: choroid plexus epithelium, intermediate zone, subventricular zone and ventricular
347 zone (30). Interestingly, low RNA levels were detected in different muscle types (Figure 5 –
348 Figure Supplement 1A). This might suggest that hypotonia in most of the patients (Table 1) is
349 most likely caused by malfunctioning of the neuronal innervation of the skeletal muscles,
350 probably related to a cerebellar defect. Taken together, the expression data of TRPM3 in the
351 central nervous system (CNS) points towards an important role of the channel in specific
352 brain regions, both in the early developmental and adult stage.
353 As it is known in some other congenital ataxia, we observed that cerebellar atrophy could be
354 progressive in a patient who has a clinically non-progressive disorder. This should encourage
355 repetition of brain imaging in the early years of life in ataxic children. Although clinical
356 variability, even intra-familial, is observed with the same mutation, we point on some
357 possible genotype-phenotype correlation to be confirmed in larger series, with
358 p.(Gly1007Ser) being associated with a milder phenotype and p.(Asn1126Asp) with a more
359 severe phenotype.
360 Functional characterization of the newly identified *TRPM3* variants revealed a pronounced
361 gain-of-function phenotype for all variants in the heterozygous (WT + mutant) condition.
362 Typically, cells expressing these variants along with the wild-type channel displayed an
363 elevated intracellular calcium concentration and increased calcium responses upon
364 stimulation with PS. These characteristics are consistent with the previously described gain-
365 of-function *TRPM3* variants p.(Val1002Met) and p.(Pro1102Gln) (14, 15).
366 The different disease-associated gain-of-function variants occur in different parts of the
367 TRPM3 channel, including the cytosolic N-terminus, the transmembrane region and the
368 cytosolic C-terminus, suggesting that they increase channel activity via distinct mechanisms
369 (Figure 1 – Figure Supplement 2). Based on fluorescent tagging of the channels, we can
370 exclude increased protein expression levels as an underlying mechanism, suggesting that the
371 variants affect channel gating or membrane localization (Figure 3 – Figure Supplement 4). In
372 this respect, it is interesting to note that, when mapped on the recent cryo-EM structure of
373 TRPM3, the affected residues L769, V1002, G1007, N1126, S1133 cluster at the interface

374 between the transmembrane domain and the cytosol, in the gating of TRPM3 and related
375 channels with six transmembrane domains (Figure 1 – Figure supplement 2) (33). The D614V
376 variant is located adjacent to exon 17, in a region that is not resolved in the cryo-EM
377 structures of the entire TRPM3 channel but forms the N-terminal interaction site for the
378 binding of the $G_{\beta\gamma}$ subunits of trimeric G proteins, leading to channel inhibition (34-36).
379 Intriguingly, our previous results showed a reduced sensitivity towards $G_{\beta\gamma}$-dependent
380 modulation for the p.(Val1002Met) variant compared to WT transfected cells (14). Further
381 work will be needed to clarify whether increased activation of the D614V variant occurs
382 (partly) via disturbed binding of the $G_{\beta\gamma}$ subunits. Interestingly, there are known mutations in
383 the upstream genetic component guanine nucleotide-binding protein beta 1 (GNB1) causing
384 severe neurodevelopmental disability, hypotonia, and seizures (37). In addition, other
385 mutations in GNB2 (38) and GNB5 (39) are observed in patients with neurodevelopmental
386 disorders. Potentially, these neurodevelopmental phenotypes could be partially be explained
387 via dysregulation of downstream TRPM3 activity.
388 Notably, L769V was the only variant that exhibited no functional activity when expressed in
389 the absence of wild-type channel subunits, whereas it caused a gain-of-function in the
390 presence of wild-type subunits, which corresponds to the situation in the cells of the
391 heterozygous patients. One possible explanation could be that the variation in the N-
392 terminus affects proper trafficking of the homotetrameric channel to the plasma membrane,
393 and that this trafficking deficit can be rescued by heteromeric channels composed of WT and
394 variant subunits. Clearly, further research is needed to pinpoint the molecular and cellular
395 mechanisms that lead to the gain-of-function caused by the channel variants, and to reveal
396 the pathophysiological mechanisms whereby altered channel function leads to the complex
397 symptoms encountered by the patients.
398 Importantly, the increased channel activity under basal conditions and associated increased
399 basal calcium levels observed with all the characterized disease-associated *TRPM3* variants
400 can be blocked by application of a high dose of the antiepileptic drug primidone, which has
401 been identified as a direct TRPM3 antagonist in *in vitro* studies and in animal models (24).
402 Since plasma levels in subjects taking primidone are expected to be sufficiently high to cause
403 significant inhibition of TRPM3 activity, it will be of great interest to evaluate whether the
404 drug can alleviate or revert symptoms in patients carrying disease-associated *TRPM3*
405 variants.

406 Taken together, we have described seven novel variants in patients with a *TRPM3*-associated
407 neurodevelopmental syndrome. The clinical phenotype of these patients is variable, with
408 global developmental delay and intellectual disability as consistent features. Epileptic
409 seizures, skeletal anomalies and pain insensitivity are observed in a subset of patients, and
410 more than half of the patients presented with a cerebellar phenotype (ataxia or severe
411 hypotonia, nystagmus or abnormal oculomotricity), associated with a progressive cerebellar
412 atrophy. We propose that *TRPM3* should be added in NGS panels designed for the diagnosis
413 of epilepsy, intellectual disability and congenital ataxia. The disease-associated variants
414 consistently result in a pronounced gain of channel function, providing strong support for
415 the hypothesis that increased channel activity, potentially leading to neuronal
416 hyperexcitability and cellular calcium overload, underlies a spectrum of TRPM3
417 channelopathies.

418 **MATERIALS and METHODS**

419 **Patient recruitment and genomic sequencing**

420 Patients with *TRPM3* variants were recruited through GeneMatcher (40) or previous
421 collaboration between the participating teams. Clinical data of each patient as well as brain
422 images were reviewed by the clinicians (geneticists, neuropediatricians, radiologists) from
423 the participating centers. Sequencing and genetic analyses were performed in the respective
424 centers on a clinical basis. The study was performed in accordance with the guidelines
425 specified by the institutional review boards and ethics committees at each institution. In
426 seven patients, trio whole exome sequencing (WES) was performed (patients 1, 2, 5, 6, 8-
427 10), while comprehensive multi-gene panel (NGS targeted panel analysis) was performed in
428 three other patients (patients 3, 4, 7). Confirmation of the variants was performed using
429 targeted Sanger sequencing in probands and parents. All parents agreed on sharing and
430 publishing the patients data.

431 **Ethics statement**

432 Patient 1, 3, 4, 7: For this patient clinical genetic services and a genetic testing was done as part of
433 routine clinical care. Written informed consent was obtained from the parents of the probands for
434 molecular genetic analysis and possible publication of the anonymized clinical data. The study was
435 done in accordance with local research and ethics requirements. Patient 2: Parents signed an
436 informed consent, received a genetic counselling before and after the analysis, and the genetic study
437 was performed in accordance with German and French ethical requirements and laws. Data sharing
438 was performed using anonymized genetic and clinical information. Patient 5: The patient was
439 identified via the Deciphering Developmental Disorders (DDD) study, which was granted by the UK
440 ethical approval by the Cambridge South Research Ethics Committee (10/H0305/83). Patient 6: This
441 patient was identified through diagnostic testing as part of their routine clinical care within the UK
442 National Health Service, and so no specific institutional ethical approval was required. Patient 8:
443 Informed consent for participation was obtained from subjects themselves or, where necessary, their
444 parents. The study was completed per protocol in accordance with the Declaration of Helsinki with
445 local approval by the Children's Hospital of Philadelphia (CHOP) Institutional Review Board (IRB 15-
446 12226). Patient 9: The participating family signed the IRB research protocol of the University of
447 Pennsylvania division of Neurology. Patient 10: The participating family consisting of the mother,
448 father, and female proband, provided written consent and was enrolled into the Center for Rare
449 Childhood Disorders (C4RCD) research protocol at the Translational Genomics Research Institute
450 (TGen). Written consent for the proband under the age of 18 years was obtained from the parents.

451 The study protocol and consent documents were approved by the Western Institutional Review
452 Board (WIRB # 20120789). The retrospective analysis of epilepsy patient data was approved by the
453 local ethics committees of the Charité (approval no. EA2/084/18).
454

455 **Patient Information**

456 ***Patient 1***

457 The proband is the first child from non-consanguineous healthy parents. She has a healthy brother.
458 No medical history in the family was reported. She was born at term without significant pregnancy
459 history. Birth parameters were within normal limits. Initially, psychomotor development was
460 described as normal, with head holding before 3 months, and she was able to sit at around 8 months.
461 The first parental concerns occurred at 14 months as the first steps were abnormally unstable. A
462 neurological assessment at 2 years noted ataxic stance and gait, and dysmetria. The child evolved
463 with a motor delay, and acquired autonomous, but unsteady walking at 25 months. She evolved with
464 cerebellar motor symptoms, ataxia of stance and gait, dysmetria, adiadochokinesia, intention tremor,
465 dysarthria, and saccadic breakdown of smooth pursuit with strabismus. The onset of speech
466 appeared normally despite dysarthria. During its evolution, until the last examination at 13 years, she
467 made motor progress, walking is less ataxic, but she had persistent tremor in fine motor skills, and
468 severe dysarthria. She never had seizure. She had a neuropsychological assessment at 10 years which
469 showed mild intellectual disability (total IQ not calculable because of the heterogeneity of the
470 scores). Difficulties were more marked in executive functions (perseveration, distractibility, disorder
471 of emotion regulation) and visuospatial function. She was in normal school and had intervention aids
472 such as speech therapy, physiotherapy, adapted educational equipment. She needed help because
473 lack of autonomy and emotional immaturity. Brain MRIs performed at 3 years 8 months showed
474 cerebellar atrophy, predominant on the superior cerebellar vermis (Figure 2), which had increased at
475 10 years. Trio whole exome sequencing identified a *de novo*, heterozygous, missense variant in the
476 *TRPM3* gene (M_001366145.2:c.1841A>T; p.(Asp614Val)).
477 For this patient clinical genetic services and a genetic testing was done as part of routine clinical care.
478 Written informed consent was obtained from the parents of the probands for molecular genetic
479 analysis and possible publication of the anonymized clinical data. The study was done in accordance
480 with local research and ethics requirements.

481 ***Patient 2***

482 She was born from healthy unrelated parents. Pregnancy, delivery and birth parameters were
483 normal. Poor visual contact was noticed in the first month of life. Ophthalmological examination
484 revealed a severely reduced central visual acuity, photophobia, normal funduscopy and a mitigated

485 photopic and scotopic ERG responses with normal flash evoked visual responses. These findings were
486 compatible with a mainly central retinal dysfunction. She also had a Mittendorf cataract at the right
487 eye. MRI performed at 6 months was considered normal. At 11 months, she was able to smile but
488 she had axial hypotonia, poor visual contact, was unable to sit and had hand wringing. She had no
489 feeding difficulties. MRI was performed at 16 months and showed a slight enlargement of cerebellar
490 sulci. She progressed slowly and at 5 years she was able to walk with assistance, with unsteady gait.
491 She had febrile seizures. Wake EEG showed background slowing without epileptic discharges, and
492 she had some episodes of sharp waves in the fronto-central regions during the night. Head
493 circumference (HC) was at -2.5 SD. She had pes calcaneovalgus and slight dysmorphism, with wide
494 nasal bridge, thin upper lip, and pointed chin. Parents reported a low reactivity to pain when
495 specifically asked the question. At that time, MRI showed cerebellar atrophy (Figure 2), confirmed by
496 MRI at 4 years. Trio exome sequencing identified the NM_001366145.2:c.2305C>G, p.(Leu769Val) *de*
497 *novo*, heterozygous *TRMP3* missense variant.
498 Parents signed an informed consent, received a genetic counselling before and after the analysis, and
499 the genetic study was performed in accordance with German and French ethical requirements and
500 laws. Data sharing was performed using anonymized genetic and clinical information.

501 ***Patient 3***

502 Patient 3 is the second child of healthy parents. Her brother was healthy. She was born at 41 weeks
503 after an uneventful pregnancy. Her birth parameters were normal (weight 3140 g; length 48 cm; HC
504 36 cm). Left hip luxation was treated by abduction splint for 6 months. She had hypotonia and
505 feeding difficulties from the first weeks, and her development was significantly delayed. She was able
506 to attain head control and independent sitting but was never able to stand alone or walk. She had a
507 paralytic thoracolumbar kyphoscoliosis requiring surgical treatment at 15 years old. She had failure
508 to thrive, and her HC growth slowed in the first months to reach - 2 SD. At 20 years-of-age, she had
509 profound intellectual and multiple disabilities. She was able to grasp the objects with dysmetria. She
510 had no language, due to her severe intellectual deficiency and was not able to communicate even
511 through visual contact. Brainstem Auditorial Evoked Potential (BAEP) showed hearing threshold at 20
512 db on the left and 30 db on the right. She had stereotypies and she never had seizures. Sleep and
513 wake EEG were both normal (one year and 8 years). She experienced feeding difficulties with
514 selective food and insufficient weight and height gain were on going. MRI performed at 4 months
515 was normal but the following MRI at 8 month's old showed global cerebellar atrophy that became
516 marked at 8 y 6m (Figure 2) and a short corpus callosum (-3 SD). Array-CGH was normal. Analysis of
517 our NGS targeted congenital ataxia panel including *TRPM3* (panel designed after the diagnosis made
518 in patient 1 using WES), identified the NM_001366145.2:c.3004G>A, p.(Val1002Leu) variant. Parental

519 analysis confirmed that the variant was absent in both parents and occurred de novo. Parental status
520 was confirmed using 16 polymorphic markers.
521 Clinical genetic services and a genetic testing was done as part of routine clinical care. Written
522 informed consent was obtained from the parents of the probands for molecular genetic analysis and
523 possible publication of the anonymized clinical data. The study was done in accordance with local
524 research and ethics requirements.

525 ***Patient 4***

526 Patient 4 is the second child of healthy parents and has a healthy brother. Pregnancy was notable by
527 the finding of clubfeet on fetal ultrasound. Amniocentesis was performed and karyotype was normal.
528 Delivery was normal at 40 weeks of gestation and birth parameters were normal. At 3 months,
529 parents worried about a lack of visual pursuit. Complete ophthalmological examination (including
530 fundus, ERG) was normal. The child was hypotonic and was not able to hold her head at 18 months.
531 At 2 ½ years, she had growth restriction (weight and height at minus 2.5 SD) and secondary
532 microcephaly (HD minus 2.5 SD). She was still unable to sit but her tone improved slightly. She could
533 not grab but was able to hold the toy placed in contact with her hand. She had poor visual contact.
534 She babbled but was unable to pronounce words. She had no spasticity. She had no clinical seizures
535 and normal EEG at this time. Control with a 24-hour EEG recorded at 4 year-old showed discharges of
536 bi-centro-parietal spikes during wake and sleep, without electrical status epilepticus during slow-
537 wave sleep. There was no obvious motor or behavioral modification, but sometimes apneas occurred
538 at beginning of the discharges, making clinical seizures possible. Primidone was recently started,
539 however at the moment we do not have enough hindsight to judge the effectiveness of primidone.
540 MRI performed at 1 year and 4 months showed a small vermis with slight atrophy, atrophy of
541 cerebellar hemispheres, and thin brainstem with small protuberance (Figure 2). Array-CGH was
542 normal. Analysis of our NGS targeted congenital ataxia panel including *TRPM3* (panel designed after
543 the diagnosis made in patient 1 using WES), identified the NM_001366145.2:c.3005T>G;
544 p.(Val1002Gly) variant. Parental analysis confirmed that the variant was absent in both parents and
545 occurred *de novo*. Parental status was confirmed using 16 polymorphic markers.
546 Clinical genetic services and a genetic testing was done as part of routine clinical care. Written
547 informed consent was obtained from the parents of the probands for molecular genetic analysis and
548 possible publication of the anonymized clinical data. The study was done in accordance with local
549 research and ethics requirements.

550 ***Patient 5***

551 This boy is the son of patient 6. He was referred to Clinical Genetics at the age of 8 years with a
552 history of global developmental delay, nocturnal epilepsy and voracious appetite. He was born at

553 term weighing 3.09 kg following a normal pregnancy complicated only by mild pre-eclampsia from 32
554 weeks gestation and a maternal history of factor V Leiden requiring enoxaparin injections. His motor
555 milestones were delayed, sitting unaided at 12 months and walking at 20 months. He required
556 speech and language therapy from three years of age. His behavior was noted to change at around
557 13 months, becoming easily unsettled when he had previously been a placid baby. He developed
558 food-seeking behavior with lack of satiety, leading to obesity. He was noted to have small genitalia
559 and subsequently had delayed puberty with reduced testosterone levels. He has never shown any
560 aggressive behavior and has never had regression of skills. He initially attended a mainstream school
561 with support but subsequently transferred to special needs education. Seizures were first noted at
562 the age of 7 years and were only present during sleep, occurring two to three times a month and
563 gradually reducing with sodium valproate treatment, which was discontinued aged 14 years. Wake
564 EEG at 7 years showed bifrontal synchronous spike and waves discharges suggestive of epileptic
565 activity. His last seizure was at the age of 18 years. Aged 21 years, he has moderate learning
566 difficulties and attends a college for learning life skills. He has some pain and heat insensitivity. He
567 has had unilateral Perthes' disease, for which he is awaiting hip replacement surgery. MRI brain did
568 not identify any gross structural abnormalities. He had normal Fragile-X syndrome testing, normal
569 Prader-Willi syndrome methylation analysis and a normal karyotype. He additionally had normal
570 methylation testing for chromosome 14 uniparental disomy. Array CGH found a maternally inherited
571 (NCBI Build 36) 6p22.3(18155949_18237422)x3 duplication of between 81-252 kb, which was not
572 thought to account for his phenotype. Whole-exome analysis via the Deciphering Developmental
573 Disorders (DDD) project identified the *TRPM3* NM_001366145.2:c.3019G>A, p.(Gly1007Ser),
574 heterozygous variant inherited from his father.
575 The patient was identified via the Deciphering Developmental Disorders (DDD) study, which was
576 granted by the UK ethical approval by the Cambridge South Research Ethics Committee
577 (10/H0305/83).

578 ***Patient 6***

579 This man was the father of patient 5 and was referred to Clinical Genetics for investigation of his mild
580 learning difficulties. He was born at 42 weeks gestation weighing 3.36 kg following a normal
581 pregnancy. His mother had required codeine analgesia for a tooth abscess early in pregnancy. There
582 were no specific concerns regarding his motor development, although he may have sat unaided later
583 than average and never crawled. He took his first steps at one year of age and developed language at
584 a normal time. He did not display any food-seeking behavior, aggression or regression of skills. He
585 attended mainstream junior school but transferred to a special educational needs senior school. He
586 has no history of seizures. He is in paid employment, undertaking manual work in a warehouse. Heat

587 and pain insensitivity has not been formally assessed but the patient is reported not to feel hot when
588 wearing warm clothing in summer time and also has a history of picking at his toenails causing
589 traumatic dystrophy without reporting this to be painful.
590 He had normal testing for Fragile X syndrome and a normal array CGH. Trio whole-genome
591 sequencing identified the *de novo TRPM3* variant NM_001366145.2:c.3019G>A, p.(Gly1007Ser).
592 This patient was identified through diagnostic testing as part of their routine clinical care within the
593 UK National Health Service, and so no specific institutional ethical approval was required.

594 ***Patient 7***

595 She is the only child of unrelated parents. During the pregnancy, her mother was treated by anti-
596 retrovirals because of a HIV infection. Delivery and birth parameters were normal (3080g, 47.5 cm,
597 34 cm). The first concern was poor visual contact noted in the first weeks and later, a nystagmus and
598 a delayed motor development. She was able to walk unaided at 20 months. Language development
599 was only slightly delayed and her cognitive level was in normal-low range. Audiometry was normal
600 and EEG was not performed in this context. At 6 years old she was able to read but had difficulties
601 writing and with fine motor skills in general. She was unable to climb or jump like other children. At
602 examination, she had a mild ataxia, only detectable when she walked following a line on the floor,
603 mild dysmetria, and nystagmus. She also had synkinesis and a prognathism. She attended
604 mainstream school with support measures (personal school assistant, logico-mathematical
605 reeducation, psychomotricity). MRI performed at 2 years and 12 years showed a mild and localized
606 atrophy of the cerebellar hemispheres (Figure 2 – Figure Supplement 1).
607 At 16 years, weight is 48.6 kg, height 157 cm, and OFC, 54 cm. Walk has drastically improved and she
608 has a slight nystagmus. She is in good health, but had a recurrent patellar dislocation leading to the
609 consideration of surgery. She is a special unit for inclusive education in a normal high-school and
610 attends a professional training in commerce.
611 NGS targeted "cerebellar anomalies" panel identified the NM_001366145.2:c.3019G>A,
612 p.(Gly1007Ser) missense variant in *TRPM3*. Parental analysis showed that the variant was *de novo*.
613 Parental status was confirmed using 16 polymorphic markers.
614 Clinical genetic services and a genetic testing was done as part of routine clinical care. Written
615 informed consent was obtained from the parents of the probands for molecular genetic analysis and
616 possible publication of the anonymized clinical data. The study was done in accordance with local
617 research and ethics requirements.

618 ***Patient 8***

619 The patient is a 4-year-old female with global developmental delay who was born to a 32-year-old G1
620 P0-1 Ab0 woman at 39 weeks by caesarian section due to breech position. Her birth weight was 3.57

621 kg. Pre-natal period was normal. Peri-natal period was complicated with feeding difficulties and she
622 remained in the hospital for 3 days. She continued with feeding difficulties and gaining weight until 8
623 months of age. Her formula was changed to and amino acid base and she was diagnosed with
624 gastroesophageal reflux disease (GERD) and successfully treated with lansoprazole and nizatidine.
625 Her development was noted to be delayed at 3 months. She was hypotonic and had no visual
626 tracking. Her electroretinogram was abnormal and she was diagnosed with cortical visual
627 impairment, strabismus, and nystagmus. She wore corrective lenses. Her brain MRI and chromosome
628 microarray was normal. Her development has been slow but she made progress. She can grab things
629 with her hands, but her fine motor skills are poor, and she is unable to feed herself. She is unable to
630 walk but she can bear weight on her legs. She is non-verbal but uses picture cards to indicate choices
631 and can recognize more than 20 images. She has not any seizures. Her EEGs have showed generalized
632 background slowing, without epileptiform discharges (routine EEG and 26 hours video EEG). For the
633 past year or two, parents have noted episodic fluctuation in her behavior. She might be very happy
634 and playful for a week or two, and then go into a period where she is irritable, crying and is
635 inconsolable as if in pain. With these periods of extreme irritability, there is often transient
636 regression in her development. She might achieve things like standing, stepping with support, or
637 chewing her food, learning to use a spoon, and then she will stop doing these things for a while.
638 Some of the episodes have been shown to be concomitant with an infection. She has no dysmorphic
639 features, cardiac or pulmonary problems. MRI showed only bilateral, symmetric, posterior
640 periventricular non-specific white matter FLAIR hyperintensities.
641 Whole exome sequencing identified a *de novo*, heterozygous, missense variant in *TRPM3* gene
642 (NM_001366145.2:c.3376A>G; p.(Asn1126Asp)) and a *de novo*, heterozygous, missense variant in
643 *PRPH2* c. 659 G>A, p.Arg220Gln pathogenic for a recessive retinopathy and possibly responsible for a
644 macular phenotype when heterozygous.
645 Informed consent for participation was obtained from subjects themselves or, where necessary, their
646 parents. The study was completed per protocol in accordance with the Declaration of Helsinki with
647 local approval by the Children's Hospital of Philadelphia (CHOP) Institutional Review Board (IRB 15-
648 12226).

649 ***Patient 9***

650 Patient 9 is the oldest child of healthy, nonconsanguineous parents of northern European descent
651 and was delivered by an uncomplicated Caesarean section for breech presentation at 37 weeks'
652 gestation. Pregnancy was complicated by preeclampsia. She was diagnosed with bilateral hip
653 dysplasia and was in a Pavlik harness for 3 months. Shortly after birth, she was noted to have diffuse
654 hypotonia, hypoactive reflexes, and roving eye movements. Difficulty tracking visual stimuli was

noted at about 4 weeks, and ophthalmologic evaluation revealed decreased visual acuity, mild bilateral macular pigmentary changes, normal refractive indices, bilateral ptosis, and disconjugate nystagmus. By the age of 25 months, she was demonstrating few motor movements, impaired upgaze, and increased lower extremity tone. She began receiving developmental services at the age of 3 months. At the age of 10 years, she can sit unsupported, but she cannot sit independently. She can roll over. She cannot walk and does not regularly stand with support. She can reach and grab for items of interest. She can fixate on objects visually and can track them, but has been diagnosed with cortical visual impairment. She can communicate with picture cards. She has a Toby device for communication but is not proficient with this. There are some behavioral outbursts. She was diagnosed with autism spectrum disorder at age 8 years.

She initially had interruptible staring spells and episodes of lip-smacking and hand-wringing shortly after birth. She was evaluated with EEG, including a 24-hour EEG at that time, the results of which were reportedly normal. She has not had any definite clinical seizures. Her parents deny any movements suspicious for seizure, including stiffening, shaking, or staring spells. Parents also deny any repetitive, purposeless movements such as hand wringing.

On examination, she has facial dysmorphism including a short philtrum, wide nasal bridge, bulbous nose tip, and epicanthal folds. She is fed via g-tube. She is capable of visual fixation and tracking briefly and is averse to a bright light shone in her eyes. She can also blink to threat bilaterally. She has intermittent, subtle, high frequency lateral nystagmus in primary gaze and in all directions of gaze. Her muscle bulk is diffusely decreased, and she is globally hypotonic. She is unable to stand or walk. She has normal deep tendon reflexes.

MRI scans over time have demonstrated stable periventricular leukomalacia. Whole exome sequencing demonstrated a *de novo* pathogenic variant in *TRPM3* (NM_001366145.2:c.3376A>G; p.(Asn1126Asp). Exome sequencing also revealed a single *de novo* loss of function (LOF) variant (c.2659dupA; p.R887Kf*42) in *TUBGCP5,* a gene tolerant to LOF (pLi=0).

The participating family signed the IRB research protocol of the University of Pennsylvania division of Neurology.

Patient 10

The patient is a 4-year-old girl, the third child of non-consanguineous German parents. The family history was unremarkable. She was born at 40th week of gestation with a birth length of 50 cm and a birth weight of 3430 g. Her psychomotor development was delayed. At age of 12 months, she was able to sit and at age of 24 months she started to walk. At the age of 24 months, she began to speak. At the age of 2.5 years, EEG investigations indicated electrical status epilepticus during slow-wave sleep (ESES). Because of the diagnosis (TRPM3 gain-of-function mutation) and the literature showing

689 primidone as an antagonist of TRPM3, a treatment by primidone was initiated. At this time, she had
690 ataxia that improved with primidone treatment as well as EEG.
691 Physical examination at age of three years showed a height of 94 cm (+0.05 SD), a weight of 19 kg
692 (+1.81 SD), and an HFC of 51.5 cm (+1.53 SD).
693 Her facial signs included a flat midface, a flat and broad nasal bridge with a broad nasal tip, upward
694 slanting palpebral fissures, strabismus, and full lips. Her fingers were short and the metacarpal bones
695 IV and V also appeared to be short. Her toes II to V also showed brachydactyly. Cranial MRI at age
696 three years was normal. In addition she had immune thrombocytopenia and hypochromic microcytic
697 anemia.
698 Cytogenetic analysis and molecular karyotyping gave normal results. Trio exome sequencing
699 identified a *de novo* variant in *TRPM3:* NM_001366145.2:c.3397T>C, p.(Ser1133Pro).
700 The participating family consisting of the mother, father, and female proband, provided written
701 consent and was enrolled into the Center for Rare Childhood Disorders (C4RCD) research protocol at
702 the Translational Genomics Research Institute (TGen). Written consent for the proband under the
703 age of 18 years was obtained from the parents. The study protocol and consent documents were
704 approved by the Western Institutional Review Board (WIRB # 20120789). The retrospective analysis
705 of epilepsy patient data was approved by the local ethics committees of the Charité (approval no.
706 EA2/084/18).

707 **Comment on the numbering of *TRPM3* variants and DNA constructs**

708 The human *TRPM3* gene contains 28 exons, and alternative splicing of the primary
709 transcripts gives rise to a large number of splice isoforms, leading to ambiguity in the
710 numbering of gene variants. Most of the previous reports based the numbering of disease-
711 associated variants on the NM_020952.4 reference sequence (9-11, 13), including the
712 Human Gene Mutation Database (41) and OMIM (https://www.omim.org/), whereas
713 NM_001007471.2 was used as reference by others (14, 15). In this report, we based the
714 numbering of the TRPM3 variants on the Mane transcript NM_001366145.2 sequence (see
715 explanation in the section "Organization of the human *TRPM3* gene and alternative splicing
716 in the cerebellum" in Results).

717 For functional expression, we used four different wild-type TRPM3 constructs, representing
718 different splice isoforms (Figure 1 - supplement 1; Table 2) (1, 15). For single-cell calcium
719 imaging, we used the isoform corresponding to GenBank AJ505026.1, with yellow
720 fluorescence protein (YFP) directly linked to the channel's C-terminus, cloned in the pCDNA3

721 vector. For plate reader-based experiments, we used the isoform corresponding to NCBI
722 reference sequence NM_001366141.2 cloned in the pcDNA3.1(+)-N-eGFP vector. For whole-
723 cell patch-clamp experiments, we used (a) the isoform corresponding to GenBank
724 AJ505026.1 (b) the isoform corresponding to NCBI reference sequence NM_001366145.2
725 and (c) the isoform corresponding to NCBI reference sequence NM_001366147.2, both (b)
726 and (c) were cloned in the pCAGGSM2_Ires_GFP vector. Human disease-associated variants
727 were introduced using the standard PCR overlap extension method, and variant sequences
728 were verified by sequencing of the entire DNA constructs (42). As indicated in the results
729 section, variant numbering was based on the amino acid position of the mutated residue in
730 the NM_001366145.2 isoform. According to this numbering, the recurrent variant
731 p.Val1027Met will be referred to as p.Val1002Met, p.Pro1127Gln as p.Pro1102Gln and
732 p.Ser1392Thr as p.Ser1367Thr.

733 **Sequence alignment**

734 CLUSTAL Omega (1.2.4) multiple sequence alignment was used to perform the alignment
735 and to obtain the Phylogenetic Tree. Jalview (2.11.2.4) was used for visualization.

736 **Cell culture and transfection**

737 HEK293T cells (identifier ATCCCRL-3216) were kindly provided by Dr. S Roper (University of
738 Miami school of medicine Depart. of physiology and biophysics, 4044 Miami FL 33136). The
739 cells were cultured as described previously (42) and used up to passage number 25. The cells
740 were tested for the lack of mycoplasma. For patch-clamp and single-cell calcium imaging,
741 cells were transfected with 2 µg of channel cDNA using TransIT-293 transfection reagent
742 (MirusBio) (42) and analyzed 36-48 hours after transfection. For the intracellular Ca^{2+}
743 measurements using a fluorescent microplate reader, cells were transfected with 400 ng of
744 channel cDNA plus 1 µg of GCaMP6 using Effectene transfection reagent (Qiagen). When
745 indicated, to mimic heterozygous conditions, a mixture of wild-type and *TRPM3* variant
746 cDNA was used (ratio 1:1). Non-transfected (NT) HEK293T cells were used as negative
747 controls in all experiments.

748 **Calcium microfluorimetry**

749 The imaging system for standard single cell calcium measurements has been described
750 before (1). Briefly, cells were incubated with 2 µM Fura-2-acetoxymethyl ester (Thermo
751 Fisher Scientific) in 1 ml culture medium for 20-60 min at 37 °C. Fluorescent signals evoked

752 during alternating illumination at 340 and 380 nm using a Lambda XL illuminator (Sutter
753 Instrument, Novato, CA, USA) and recorded by an Orca Flash 4.0 camara (Hamamatsu
754 Photonics, Belgium) on a Nikon Eclipse Ti fluorescence microscope (Nikon Benelux, Brussels,
755 Belgium). The imaging data were recorded using NIS-element software (NIS-Elements).
756 Absolute calcium concentrations were calculated from the ratio of the fluorescence signals
757 at both wavelengths (F_{340}/F_{380}) after correction for the individual background fluorescence
758 signals, using the Grynkiewicz equation (43): $[Ca^{2+}] = K_m \times (R-R_{min})/(R_{max}-R)$, where K_m, R_{min}
759 and R_{max} were estimated from *in vitro* calibration experiments with known calcium
760 concentrations. The standard imaging solution contained (in mM): 150 NaCl, 2 $CaCl_2$, 1
761 $MgCl_2$, and 10 HEPES, pH 7.4 with NaOH (~320 mOsm). Calcium amplitudes were calculated
762 as the difference between the maximum calcium concentration during the period of
763 stimulus application and the basal value before stimulation of responding cells. At the start
764 of the recording, cellular YFP fluorescence was determined as a measure of TRPM3 protein
765 expression levels. All data represent the results from at least three independent coverslips.

766 For the intracellular Ca^{2+} measurements using a fluorescent microplate reader, HEK293T
767 cells were plated on poly-D-lysine coated black-wall clear-bottom 96-well plates after 24h of
768 transfection, and measurements were performed 24–48 h after plating. Experiments were
769 performed at room temperature in a buffer containing (in mM): 137 NaCl, 5 KCl, 1 $MgCl_2$, 2
770 $CaCl_2$, 10 HEPES and 10 glucose (pH 7.4) with NaOH. Intracellular Ca^{2+} levels were measured
771 by a Flexstation-3 96-well plate reader (Molecular Devices). GCaMP6 signal was detected at
772 excitation wavelengths 485 nm and fluorescence emission was detected at 525 nm. Various
773 concentrations of PS were applied to activate TRPM3 channels and 2 μM ionomycin was
774 applied at the end of the experiment to induce the maximum calcium influx. For every
775 experimental group, three transfections were performed and signals from 4 replicates were
776 collected for different PS concentrations within the same transfection.

777 **Electrophysiology**

778 Whole-cell patch-clamp recordings were performed using an EPC-10 amplifier and the
779 PatchMasterPro software (HEKA Elektronik). Current measurements were done at a
780 sampling rate of 20 kHz and currents were digitally filtered at 2.9 kHz. In all measurements,
781 70% of the series resistance was compensated. The standard internal solution contained (in
782 mM): 100 CsAsp, 45 CsCl, 10 EGTA, 10 Hepes, 1 $MgCl_2$ (pH 7.2 with CsOH); and the standard

783 extracellular solution contained (in mM): 150 NaCl, 1 $MgCl_2$, 10 Hepes (pH 7.4 with NaOH).
784 The standard patch pipette resistance was between 2 and 4 MΩ when filled with pipette
785 solution. All experiments were performed at room temperature (23 ± 1°C). To evaluate the
786 channel activity at basal level and in the presence of PS (40 µM), a voltage step protocol was
787 applied in which voltage steps of +40 mV were applied starting from -160 mV towards +160
788 mV with a holding potential at 0 mV.

789 **Chemicals**

790 All chemicals were obtained from Sigma-Aldrich, ionomycin was purchased from Cayman
791 Chemical. Pregnenolone sulphate (PS) and primidone were dissolved in the bath solutions
792 from a 100 mM stock diluted in DMSO.

793 **Statistics**

794 Calcium microfluorimetry data were analyzed with NIS-Elements software (Nikon, Japan),
795 Excel (Microsoft, WA, USA), IgorPro 6.2 (WaveMetrics, OR, USA) and OriginPro 9.5
796 (OriginLab, MA, USA). RStudio Team (2020) (Integrated Development for R. RStudio, PBC,
797 Boston, MA URL http://www.rstudio.com/.), GraphPad Prism (9.2.0) and OriginPro 9.5 were
798 further used for statistical analysis and data display. All data sets were tested for normality
799 using the Shapiro-Wilk test and depending on the outcome, a One-way ANOVA or a Kruskal-
800 Wallis test with subsequent Tukey's, Dunn's or Dunnett's posthoc tests were performed or a
801 two-way ANOVA with Sidak's multiple comparison was used. When having paired non-
802 normally distributed data sets, a Wilcoxon signed rank test was performed. P values below
803 0.05 were considered as significant. Data points represent means ± SEM of the given number
804 (n) of identical experiments. No exclusion of statistical outliers was performed in this study.

805 **Data Availability**

806 Data will be stored at a database controlled by the corresponding author and will become
807 freely available after contacting the corresponding author.

808 **ACKNOWLEDGEMENTS**

809 We thank all parents and children for their willingness to participate to this study. We thank
810 all members of the Laboratory of Endometrium, Endometriosis and Reproductive Medicine
811 (LEERM) and the members of the Laboratory of Ion Channel Research (LICR) Leuven for their
812 help during experiments and useful discussions. We thank Dr. L Gaspers for the kind gift on
813 GCaMP6, and Bahar Bazeli for help with visualizing the TRPM3 variants on the cryo-EM
814 structure. The study was supported by the Einstein Stiftung Fellowship through the Günter
815 Endres Fond.

DECLARATIONS

Ethics approval and consent to participate

The study was performed in accordance with the guidelines specified by the institutional review boards and ethics committees at each institution.

Consent for publication

All patient information was required after signing an institutional consent for publication.

Competing interests

The authors declare no conflict of interest.

Funding

We thank the Research Foundation-Flanders FWO, (G.0D1417N, G.084515N, G.0A6719N), the Research Council of the KU Leuven (C14/18/106, C3/21/049) for funding the project of JV, Einstein Stiftung for AMK, and the association “Connaître les syndromes cérébelleux” for funding the project of LB. EVH is a fellow of the Research Foundation-Flanders FWO (11E782N).

830 **REFERENCES**

831 1. Vriens J, Owsianik G, Hofmann T, Philipp SE, Stab J, Chen X, et al. TRPM3 is a nociceptor
832 channel involved in the detection of noxious heat. Neuron. 2011;70(3):482-94.
833 2. Wagner TF, Loch S, Lambert S, Straub I, Mannebach S, Mathar I, et al. Transient receptor
834 potential M3 channels are ionotropic steroid receptors in pancreatic beta cells. Nat Cell Biol.
835 2008;10(12):1421-30.
836 3. Su S, Yudin Y, Kim N, Tao YX, Rohacs T. TRPM3 channels play roles in heat hypersensitivity
837 and spontaneous pain after nerve injury. J Neurosci. 2021.
838 4. Vangeel L, Benoit M, Miron Y, Miller PE, De Clercq K, Chaltin P, et al. Functional expression
839 and pharmacological modulation of TRPM3 in human sensory neurons. Br J Pharmacol. 2020.
840 5. Grimm C, Kraft R, Sauerbruch S, Schultz G, Harteneck C. Molecular and functional
841 characterization of the melastatin-related cation channel TRPM3. J Biol Chem. 2003;278(24):21493-
842 501.
843 6. Oberwinkler J, Lis A, Giehl KM, Flockerzi V, Philipp SE. Alternative splicing switches the
844 divalent cation selectivity of TRPM3 channels. J Biol Chem. 2005;280(23):22540-8.
845 7. Zamudio-Bulcock PA, Everett J, Harteneck C, Valenzuela CF. Activation of steroid-sensitive
846 TRPM3 channels potentiates glutamatergic transmission at cerebellar Purkinje neurons from
847 developing rats. J Neurochem. 2011;119(3):474-85.
848 8. Rauch A, Wieczorek D, Graf E, Wieland T, Endele S, Schwarzmayr T, et al. Range of genetic
849 mutations associated with severe non-syndromic sporadic intellectual disability: an exome
850 sequencing study. Lancet. 2012;380(9854):1674-82.
851 9. de Sainte Agathe JM, Van-Gils J, Lasseaux E, Arveiler B, Lacombe D, Pfirrmann C, et al.
852 Confirmation and Expansion of the Phenotype Associated with the Recurrent p.Val837Met Variant in
853 TRPM3. Eur J Med Genet. 2020;63(8):103942.
854 10. Dyment DA, Terhal PA, Rustad CF, Tveten K, Griffith C, Jayakar P, et al. De novo substitutions
855 of TRPM3 cause intellectual disability and epilepsy. Eur J Hum Genet. 2019;27(10):1611-8.
856 11. Gauthier LW, Chatron N, Cabet S, Labalme A, Carneiro M, Poirot I, et al. Description of a
857 novel patient with the TRPM3 recurrent p.Val837Met variant. Eur J Med Genet. 2021;64(11):104320.
858 12. Kang Q, Yang L, Liao H, Yang S, Kuang X, Ning Z, et al. A Chinese patient with developmental
859 and epileptic encephalopathies (DEE) carrying a TRPM3 gene mutation: a paediatric case report. BMC
860 Pediatr. 2021;21(1):256.
861 13. Lines MA, Goldenberg P, Wong A, Srivastava S, Bayat A, Hove H, et al. Phenotypic spectrum
862 of the recurrent TRPM3 p.(Val837Met) substitution in seven individuals with global developmental
863 delay and hypotonia. Am J Med Genet A. 2022.
864 14. Van Hoeymissen E, Held K, Nogueira Freitas AC, Janssens A, Voets T, Vriens J. Gain of channel
865 function and modified gating properties in TRPM3 mutants causing intellectual disability and
866 epilepsy. Elife. 2020;9.
867 15. Zhao S, Yudin Y, Rohacs T. Disease-associated mutations in the human TRPM3 render the
868 channel overactive via two distinct mechanisms. Elife. 2020;9.
869 16. Behrendt M, Gruss F, Enzeroth R, Dembla S, Zhao S, Crassous PA, et al. The structural basis
870 for an on-off switch controlling Gbetagamma-mediated inhibition of TRPM3 channels. Proc Natl Acad
871 Sci U S A. 2020;117(46):29090-100.
872 17. Held K, Aloi VD, Freitas ACN, Janssens A, Segal A, Przibilla J, et al. Pharmacological properties
873 of TRPM3 isoforms are determined by the length of the pore loop. Br J Pharmacol. 2020.
874 18. Held K, Kichko T, De Clercq K, Klaassen H, Van Bree R, Vanherck JC, et al. Activation of TRPM3
875 by a potent synthetic ligand reveals a role in peptide release. Proc Natl Acad Sci U S A.
876 2015;112(11):E1363-72.
877 19. Held K, Toth BI. TRPM3 in Brain (Patho)Physiology. Front Cell Dev Biol. 2021;9:635659.
878 20. Vriens J, Held K, Janssens A, Toth BI, Kerselaers S, Nilius B, et al. Opening of an alternative ion
879 permeation pathway in a nociceptor TRP channel. Nat Chem Biol. 2014;10(3):188-95.

880 21. Lines MA, Goldenberg P, Wong A, Srivastava S, Bayat A, Hove H, et al. Phenotypic spectrum
881 of the recurrent TRPM3 p.(Val837Met) substitution in seven individuals with global developmental
882 delay and hypotonia. Am J Med Genet A. 2022;188(6):1667-75.
883 22. Quang D, Chen Y, Xie X. DANN: a deep learning approach for annotating the pathogenicity of
884 genetic variants. Bioinformatics. 2015;31(5):761-3.
885 23. Zhao C, MacKinnon R. Structural and functional analyses of a GPCR-inhibited ion channel
886 TRPM3. Neuron. 2022.
887 24. Krugel U, Straub I, Beckmann H, Schaefer M. Primidone inhibits TRPM3 and attenuates
888 thermal nociception in vivo. Pain. 2017;158(5):856-67.
889 25. Leto K, Arancillo M, Becker EB, Buffo A, Chiang C, Ding B, et al. Consensus Paper: Cerebellar
890 Development. Cerebellum. 2016;15(6):789-828.
891 26. Sathyanesan A, Zhou J, Scafidi J, Heck DH, Sillitoe RV, Gallo V. Emerging connections between
892 cerebellar development, behaviour and complex brain disorders. Nat Rev Neurosci. 2019;20(5):298-
893 313.
894 27. Schmahmann JD. The cerebellum and cognition. Neurosci Lett. 2019;688:62-75.
895 28. Hoffmann A, Grimm C, Kraft R, Goldbaum O, Wrede A, Nolte C, et al. TRPM3 is expressed in
896 sphingosine-responsive myelinating oligodendrocytes. J Neurochem. 2010;114(3):654-65.
897 29. Oberwinkler J, Philipp SE. Trpm3. Handb Exp Pharmacol. 2014;222:427-59.
898 30. Aldinger KA, Thomson Z, Phelps IG, Haldipur P, Deng M, Timms AE, et al. Spatial and cell type
899 transcriptional landscape of human cerebellar development. Nat Neurosci. 2021;24(8):1163-75.
900 31. Lake BB, Chen S, Sos BC, Fan J, Kaeser GE, Yung YC, et al. Integrative single-cell analysis of
901 transcriptional and epigenetic states in the human adult brain. Nat Biotechnol. 2018;36(1):70-80.
902 32. Velmeshev D, Schirmer L, Jung D, Haeussler M, Perez Y, Mayer S, et al. Single-cell genomics
903 identifies cell type-specific molecular changes in autism. Science. 2019;364(6441):685-9.
904 33. Owsianik G, D'Hoedt D, Voets T, Nilius B. Structure-function relationship of the TRP channel
905 superfamily. Rev Physiol Biochem Pharmacol. 2006;156:61-90.
906 34. Badheka D, Yudin Y, Borbiro I, Hartle CM, Yazici A, Mirshahi T, et al. Inhibition of Transient
907 Receptor Potential Melastatin 3 ion channels by G-protein betagamma subunits. Elife. 2017;6.
908 35. Dembla S, Behrendt M, Mohr F, Goecke C, Sondermann J, Schneider FM, et al. Anti-
909 nociceptive action of peripheral mu-opioid receptors by G-beta-gamma protein-mediated inhibition
910 of TRPM3 channels. Elife. 2017;6.
911 36. Quallo T, Alkhatib O, Gentry C, Andersson DA, Bevan S. G protein betagamma subunits inhibit
912 TRPM3 ion channels in sensory neurons. Elife. 2017;6.
913 37. Petrovski S, Kury S, Myers CT, Anyane-Yeboa K, Cogne B, Bialer M, et al. Germline De Novo
914 Mutations in GNB1 Cause Severe Neurodevelopmental Disability, Hypotonia, and Seizures. Am J Hum
915 Genet. 2016;98(5):1001-10.
916 38. Fukuda T, Hiraide T, Yamoto K, Nakashima M, Kawai T, Yanagi K, et al. Exome reports A de
917 novo GNB2 variant associated with global developmental delay, intellectual disability, and
918 dysmorphic features. Eur J Med Genet. 2020;63(4):103804.
919 39. Lodder EM, De Nittis P, Koopman CD, Wiszniewski W, Moura de Souza CF, Lahrouchi N, et al.
920 GNB5 Mutations Cause an Autosomal-Recessive Multisystem Syndrome with Sinus Bradycardia and
921 Cognitive Disability. Am J Hum Genet. 2016;99(3):704-10.
922 40. Sobreira N, Schiettecatte F, Valle D, Hamosh A. GeneMatcher: a matching tool for connecting
923 investigators with an interest in the same gene. Hum Mutat. 2015;36(10):928-30.
924 41. Stenson PD, Mort M, Ball EV, Evans K, Hayden M, Heywood S, et al. The Human Gene
925 Mutation Database: towards a comprehensive repository of inherited mutation data for medical
926 research, genetic diagnosis and next-generation sequencing studies. Hum Genet. 2017;136(6):665-
927 77.
928 42. Vriens J, Owsianik G, Janssens A, Voets T, Nilius B. Determinants of 4 alpha-phorbol
929 sensitivity in transmembrane domains 3 and 4 of the cation channel TRPV4. J Biol Chem.
930 2007;282(17):12796-803.

931 43. Grynkiewicz G, Poenie M, Tsien RY. A new generation of Ca2+ indicators with greatly
932 improved fluorescence properties. J Biol Chem. 1985;260(6):3440-50.

933 **TABLE 1: Overview patient information**

Patient	1	2	3	4	5 (Son of 6)	6 (Father of 5)	7	8	9	10
Method	Exome trio	Exome trio	Panel NGS	Panel NGS	Exome trio	Genome trio	Panel NGS	Exome trio	Exome trio	Exome trio
Age at last examination	13 years	7.5 years	20 years	30 months	21 years	45 years	16 years	4 years	10 years	3 years
Sex	F	F	F	F	M	M	F	F	F	F
OFC (SD)	0	- 2.5	- 2	- 2.5	M	M	- 1	- 1.8	+ 1	+ 1.5
Height (SD)	0	na	- 3	- 2.5	+ 0.5	+ 0.5	- 1.8	96.5 cm	na	0
Weight (SD)	+ 0.5	na	na	- 2.5	<+ 5	0	na	16 kg	- 0.5	+ 1.8
Pregnancy or delivery event	No	Placenta accreta	No	Club foot	Mild pre-eclampsia	Reduced fetal movements	No	C-section Breech position	Pre-eclampsia C-section	No
Maternal treatment	No	No	No	No	Enoxaparin injections	Codeine –tooth abscess	Antiretroviral therapy	No	No	Heparine therapy
Birth (weeks)	40	Full term	41	40	Full term	42	na	39	37	40
Birth OFC (cm)	33.5	na	36	34.5	na	na	34	35.6	na	na
Birth weight (g)	3020	3500	3140	3150	3090	3360	3080	3570	2637	3430
Birth length (cm)	44	na	48	47	na	na	47.5	50.8	na	50
First signs (age)	Unstable gait (14 months)	Poor visual contact (1month)	Hypotonia, poor visual contact (first weeks)	Lack of visual pursuit (3 months)	Motor delay (first months)	Mild learning difficulties	Poor visual contact (first weeks), abnormal ocular movements	Feeding difficulties hypotonia and no visual tracking (3 months)	Neonatal hypotonia, abnormal ocular movements	Motor delay (first months)
Hypotonia first months	No	Yes	Yes	Yes	Yes	Yes	Yes	Yes	Yes	No
Achieved psychomotor milestones	Able to walk unaided (ataxic)	Able to walk with aid	Able to sit, hypotonia, moves on the buttocks, poor visual contact	Unstable head, hypotonia, unable to follow	Able to walk unaided after motor delay	Able to sit unaided with delay	Able to walk unaided after motor delay	Unable to walk	Unable to walk	Able to sit: 12 months
Walking age	25 m (ataxic)	4 years with aid	Not acquired	Not acquired	19 months	Normal	20 months	Not acquired	Not acquired	24 months
Ataxia	Yes	Yes	Severe hypotonia	Na	No	No	Yes , improving; at 16: very mild	Na (unable to walk)	No	Yes
Tremor	Yes	No	No	No	No	No	Yes (hands)	No	No	No
Dysmetria	Yes	na	na	na	No	No	Very mild, adiadococinesia	Yes	No	na
Dysarthria	Yes	na	na	na	No	No	na	Non-verbal	No	na

Dystonia	No	na	Yes	No	No	No	hand "crispation"	No	na	No
Abnormal movements	Myoclonies	na	Saccadic gesticulation	No	No	No	Syncinesia	Stereotyped hand movement	na	Ataxia
Amyotrophy	Yes	na	na	na	na	na	na	na	na	No
Epilepsy (age, treatment)	No	Febrile seizures (5 years, no treatment)	No	Doubtful seizures, abundant interictal discharges (4y, primidone)	Nocturnal epilepsy generalised tonic-clonic (7 years, no treatment)	No	No	Doubtful	Neonatal episodes (uncertain)	Yes (30 m, primidone)
EEG: age/ findings/ (Wake W/Sleep S)	na	5 years: Background slowing (W); episodes of sharp waves in the fronto-central regions (S)	1/8 years: Normal (W/S)	30 months: Normal EEG 4y: Background slowing, alpha central since 6m, biparietal spikes, no ESES (W/S)	7 years: bifrontal synchronous spike and waves discharges (W)	na	na	3 years: Generalized - background slowing, no eptileptic dicharges (W/S)	Several before 10 years: Normal (W/S)	2.5 years: ESES (W/S)
Pain insensitivity (Y/N)?	No	Yes	na	na	Yes	Yes	na	na	No	Yes
Heat insensitivity	No	No	na	na	No	Yes	na	Yes	No	na
Language	Normal	Monosyllabic	Absent	Absent	Delayed	Normal	Slightly delayed then normal	Non-verbal (picture cards)	Non-verbal (picture cards)	Delayed
Intellectual deficiency	Normal low/mild ID	Severe-moderate	Severe	Probably severe	Moderate	Mild	Very mild-low normal	Moderate	Severe	Yes
Behavior anomalies	No	No	No	No	Food-seeking	No	No	Yes	Occasional outbursts, stereotypies ***	Aggressivity
Autism spectrum disorder (Y/N)?	No	No	Poor contact (severe ID)	Poor contact (severe ID)	No	No	No	No	Yes	Yes
School	Special school (attention deficit, slow)	Specialized institution	Institution for children with profound intellectual and multiple disabilities	na	Special education	Normal then special education	Mainstream school with support measures, able to read, writing difficulties, slow	Foundation for Blind School making slow progress	na	na
Evolution	Progress	Progress	Stable	Stable	Progress	Progress	Progress	Progress but episodes of mild psychomotor regression concomitant with	na	Progress

								behavioral fluctuations -		
Ocular anomalies	Strabismus, saccadic breakdown of smooth pursuit	Abnormal eye pursuit	Strabismus	No	Hypermetropia, left convergent squint	No	Nystagmus	Cortical visual impairment, nystagmus, strabismus	Disconjugate nystagmus	Strabismus
Skeletal anomalies	12th hypoplastic rib pair	Pes calcaneovalgus	Congenital hip luxation – later paralytic kyphoscoliosis	na	Left Perthes' disease	No	Valgus foot, patellar dislocation	No	Hip dysplasia	Brachydactyly
Others					Small genitalia, delayed puberty, gynecomastia	Skin tags, dry palmar skin	Prognathism	Failure to thrive, (milk protein allergy, GERD)	Feedings difficulties G-tube fed	Immune thrombocytopenia and hypochromic microcytic anemia
MRI (age)	3y 8m: cerebellar atrophy, increased at 10 years	6 m: normal 2 y 2 m: cerebellar vermis and hemispheres atrophy	4 m: "normal" 8 m: brainstem and cerebellar atrophy, short corpus callosum	1y 4 m: brainstem and cerebellar atrophy	Normal	Not done*	Very mild localized atrophy of cerebellar hemispheres	Normal	Not done**	Normal (3y)
Mutation NM_001366145.2	c.1841A>T p.(Asp614Val)	c.2305C>G p.(Leu769Val)	c.3004G>T p.(Val1002Leu)	c.3005T>G p.(Val1002Gly)	c.3019G>A p.(Gly1007Ser)	c.3019G>A p.(Gly1007Ser)	c.3019G>A p.(Gly1007Ser)	c.3376A>G p.(Asn1126Asp)	c.3376A>G p.(Asn1126Asp)	c.3397T>C p.(Ser1133Pro)
Inheritance	de novo	de novo	de novo	de novo	Inherited from the father	de novo	de novo	de novo	de novo	de novo

ESES: Electrical status epilepticus during slow-wave sleep

*TDM normal

**Cerebral TDM at 5 y: Periventricular white matter loss.

***(repetitive hyperventilation)

939 **TABLE 2: Overview used splice isoforms**

Splice isoform	Start	Exon 8	Exon 15	Exon 17	Exon 24	Exon 28	Functionality*
AJ505026.1	Exon 2	-	-	+	short	spliced	Normal
NM_001366141.2	Exon 1	-	-	+	short	full	Normal
NM_001366145.2	Exon 2	-	+	+	short	full	Normal
NM_001366147.2	Exon 2	+	+	+	short	full	No activity

940 *Normal functionality refers to whole-cell currents activated by ligands including PS,
941 CIM0216 and clotrimazole, with biophysical properties as described in Held et al. (18) and
942 Vriens et al. (20).

943 **TABLE 3: Characteristics of the variants**

944

Variant	gnomAD	SIFT	CADD	PROVEAN	DANN
c.1841A>T p.(Asp614Val)	absent	deleterious	25.3	damaging	0.9865
c.2305C>G p.(Leu769Val)	absent	tolerated	25.9	damaging	0.9986
c.3004G>T p.(Val1002Leu)	absent	tolerated	24.8	damaging	0.9969
c.3005T>G p.(Val1002Gly)	absent	deleterious	26.3	damaging	0.9973
c.3019G>A p.(Gly1007Ser)	absent	deleterious	27.8	damaging	0.9986
c.3376A>G p.(Asn1126Asp)	absent	tolerated	28.4	damaging	0.9977
c.3397T>C p.(Ser1133Pro)	absent	deleterious	27.2	damaging	0.9987

945

946

947

948

949

950 Characteristics of the variants (database, predicted pathogenicity). Overview of the different

951 variants and the identification protocol.

952 **FIGURE LEGENDS**

953 **Figure 1: Overview of the *TRPM3* gene and location of the different variants.**
954 (**A**), Exon-intron structure and alternative splicing of *TRPM3*. Percentages above colored
955 exons indicate the percentage of transcripts that include the indicated exons in human
956 cerebellar RNA-seq analyses. Exons included for numbering of the disease-associated
957 variants are indicated in grey, blue and green, resulting in the functional channel construct
958 indicated in (**B**). Variant numbering was based on the amino acid position of the mutated
959 residue in the NM_001366145.2 isoform. See text for more details.
960

961 **Figure 2: Successive MRI images of several patients carrying different *TRPM3* variants.**
962 ***** normal MRI: the fissures of the vermis and cerebellar hemispheres are nearly virtual. (**A**-**I**)
963 MRI of the patients showing variable widening of the cerebellar fissures (arrows) reflecting
964 cerebellar (vermis and/or hemispheres) atrophy. (**A**-**D**) Patient 1, MRI at 3 years 8 months
965 showing slight atrophy of the vermis (a-sagittal T1) and cerebellar hemispheres (B-coronal
966 T1); and majoration of the atrophy at 10 years (c-sagittal T1 and d-coronal T2), (**E-F)** Patient
967 3; MRI at 8 years 6 months: severe atrophy of the vermis (arrow) and brainstem (star), and
968 atrophy of the cerebellar hemispheres (sagital and coronal T1). (**G**-**J**)successive MRIs in
969 patient showing progressive atrophy (g:2y 2m; h: 6m; i-j: 4y 2m). (**K**, **L**) Patient 4; MRI at 1y
970 4m: small vermis, thin brainstem (star) and atrophy of the cerebellar hemispheres (sagittal
971 and coronal T1).
972

973 **Figure 3: Homozygous mutant expression in HEK293T cells**.
974 (**A**) Time course of intracellular calcium concentrations ($[Ca^{2+}]_i$) (± SEM) upon application of
975 the TRPM3 inhibitor primidone (100 µM) for wild-type (WT; black) (n=449), and homozygous
976 V1002M (green) (n=271), V1002G (blue) (n=257) and G1007S (red) (n=409) transfected
977 HEK293T cells, and non-transfected (NT; grey) (n=982) (N=3 independent measurements).
978 (**B**) Mean basal intracellular calcium concentrations, $[Ca^{2+}]_I$, in the absence (full bars) and
979 presence of primidone (100 µM) (striped bars). Data are represented as mean ± SEM, using a
980 two-way ANOVA with Sidak's posthoc test. P-values of baseline vs WT: NT (p=0.8376), D614V
981 (p<0.0001), L794V (p>0.9999), V1002M (p<0.0001), V1002G (p<0.0001), V1002L (p<0.0001),
982 G1007S (p<0.0001), P1102Q (p=0.0018), N1126D (p<0.0001), S1133P (p<0.0001); p-values

983 baseline vs primidone: NT (p>0.9999), WT (p=0.9994), D614V (p<0.0001), L794V (p>0.9999),
984 V1002M (p<0.0001), V1002G (p<0.0001), V1002L (p<0.0001), G1007S (p=0.5663), P1102Q
985 (p=0.0138), N1126D (p<0.0001), S1133P (p<0.0001). (**C**) Time course of $[Ca^{2+}]_I$ (± SEM) for
986 wild-type (WT; black) (n=243), D614V (green) (n=220), L794V (blue) (n=420) and V1002L
987 (red) (n=264) transfected HEK293T cells, and non-transfected (NT; grey) (n=452) upon
988 application of pregnenolone sulphate (PS; 40 µM) (N=3 independent measurements). (**D**)
989 Corresponding calcium amplitudes of the PS response, represented as mean ± SEM, using a
990 Kruskal-Wallis ANOVA with Dunnett's posthoc test (p-values vs WT: D614V (p<0.0001),
991 L794V (p<0.0001), V1002M (p<0.0001), V1002G (p<0.0001), V1002L (p<0.0001), G1007S
992 (p=0.0006), P1102Q (p=0.0102), N1126D (p=0.0098), S1133P (p<0.0001)). For these
993 experiments, the isoform corresponding to GenBank AJ505026.1 was used.
994
995 **Figure 4**: **Heterozygous mutant + WT expression in HEK293T cells**.
996 (**A**) Time course of $[Ca^{2+}]_I$ ± SEM upon application of the TRPM3 inhibitor primidone (100
997 µM) for wild-type (WT; black) (n=449), and heterozygous WT + V1002M (green) (n=373), WT
998 + V1002G (blue) (n=482) and WT + G1007S (red) (n=561) transfected HEK293T cells, and
999 non-transfected (NT; grey) (n=982) (N= 3 independent measurements). (**B**) Mean basal
1000 $[Ca^{2+}]_I$ ± SEM in the absence (full bars) and presence of primidone (striped bars). A two-way
1001 ANOVA with Sidak's posthoc test was used. P-values of baseline vs WT: NT (p=0.6733),
1002 D614V (p<0.0001), L794V (p<0.0001), V1002M (p<0.0001), V1002G (p<0.0001), V1002L
1003 (p<0.0001), G1007S (p<0.0001), P1102Q (p=0.9249), N1126D (p=0.5539), S1133P (p<0.0001);
1004 p-values baseline vs primidone: NT (p>0.9999), WT (p=0.9994), D614V (p<0.0001), L794V
1005 (p<0.0001), V1002M (p<0.0001), V1002G (p<0.0001), V1002L (p<0.0001), G1007S
1006 (p<0.0001), P1102Q (p=0.8205), N1126D (p=0.5132), S1133P (p<0.0001). (**C**) Time course of
1007 $[Ca^{2+}]_I$ (±SEM) for wild-type (WT; black) (n=243), WT + D614V (green) (n=281), WT + L794V
1008 (blue) (n=497) and WT + V1002L (red) (n=276) transfected HEK293T cells, and non-
1009 transfected (NT; grey) (n=452) upon application of PS (40 µM) (N= 3 independent
1010 measurements). (**D**) Corresponding calcium amplitudes of the PS response, represented as
1011 mean ± SEM, using a Kruskal-Wallis ANOVA with Dunnett's posthoc test (p-values vs WT:
1012 D614V (p<0.0001), L794V (p<0.0001), V1002M (p<0.0001), V1002G (p=0.0155), V1002L
1013 (p<0.0001), G1007S (p<0.0001), P1102Q (p=0.0564), N1126D (p=0.0277), S1133P

1014 (p<0.0001)). For these experiments, the isoform corresponding to GenBank AJ505026.1 was
1015 used.
1016

1017 **Figure 5**: **TRPM3 expression in the human cerebellum.**
1018 (**A,B**) UMAP visualization of human cerebellar nuclei annotated on the basis of marker genes
1019 for the developing (A) and adult cerebellum (B). (**C, D**) The same UMAP visualization of
1020 human cerebellar nuclei as panel (A) and (B), now representing the expression of TRPM3 for
1021 the developing (C) and adult cerebellum (D), respectively. (**E,F**) Dot plot showing the
1022 expression of one selected marker gene per cell type for the developing (E) and adult
1023 cerebellum (F). The size of the dot represents the percentage of nuclei within a cell type in
1024 which that marker was detected and its color represents the average expression level. (**G**)
1025 Dot plot showing the expression of one selected marker gene per region of the rhombic lip
1026 (RL). Data set of TRPM3 in developing cerebellum adapted from (30). Data set of TRPM3 in
1027 adult cerebellum adapted from (31).

1028 **SUPPLEMENTARY FIGURES LEGENDS**

1029 **Figure 1 – Figure supplement 1**: **Functional characterization of different human TRPM3**
1030 **constructs**. (**A-B**) Three different variants of human *TRPM3* (AJ505026.1 (black, n=416 cells),
1031 NM_001366145.2 (dark grey, n=673), and NM_001366147.2 (light grey, n=644) were
1032 functionally characterized via Fura-2 fluorimetric experiments (N ≥ 3 independent
1033 experiments). The TRPM3 agonist pregnenolone sulphate (PS; 40 µM) and clotrimazole (Clt;
1034 10 µM) were applied at the indicated time periods. (B) Corresponding calcium amplitudes
1035 after stimulation by PS, clotrimazole (Clt) and co-application of PS+Clt, represented as mean
1036 ± SEM. (**C**-**D**) NM_001366145.2 construct was further characterized via whole-cell patch-
1037 clamp experiments in HEK293T cells (N = 5) after stimulation by PS (40 µM), clotrimazole
1038 (Clt; 10 µM) and co-application PS+Clt. (C) Time course of whole-cell patch clamp recording
1039 at holding of +150 mV (open circles) and -150 mV (closed circles) of HEK293T cells expressing
1040 the TRPM3 NM_001366145.2 construct. (D) Current-voltage relationship of time points
1041 indicated in panel (C).

1042

1043 **Figure 1 – Figure supplement 2**: **Structural model of TRPM3 based on the cryo-EM**
1044 **structure (pdb: 8DDQ)**

1045 (**A-B**) Structural model of TRPM3, based on the cryo-EM structure (pdb: 8DDQ), seen from
1046 the side (A) and the top (B), indicating residues that are altered in the disease-associated
1047 variants. In one of the four subunits (blue), the red circled area indicates the location of the
1048 non-resolved loop where D694 is located, close to the interaction site of $G_{\beta\gamma}$. Other affected
1049 residues are indicated in magenta and green. (**C**) A cluster of disease-associated residues
1050 (magenta) is localized at the interface between transmembrane domain and cytosol,
1051 whereas P1092 is located at the extracellular part of transmembrane helix S6.

1052

1053 **Figure 1 - Figure supplement 3: Sequence alignment of TRPM3 with different species and**
1054 **different members of the TRP melastatin (M) family.**

1055 CLUSTAL Omega (1.2.4) multiple sequence alignment was used to perform the alignment
1056 and to obtain the Phylogenetic Tree as shown on the left top. Sequence alignment at
1057 position D614, L769, V1002, G1007, P1102, N1126, S1133 is conserved across multiple
1058 species (**A**) and conserved across related members of the TRPM family (**B**).

1059

1060 **Figure 2 - Figure supplement 1**: **MRI of patient 7 and patient 8**
1061 (**A**-**B**) Patient 7, very mild and localized atrophy of the cerebellar hemispheres (arrows),
1062 stable (2 years 10 months (A); 12 years 1 month (B)). (**C**) Patient 8, normal posterior fossa at
1063 age of 3 years; non-specific bilateral symmetric periventricular white matter hyperintensities
1064 on FLAIR axial MRI (arrows).
1065
1066 **Figure 3 – Figure Supplement 1: Elevated basal activity in HEK293T cells expressing TRPM3**
1067 **variants.** Time course of intracellular calcium concentrations, $[Ca^{2+}]_I$ ± SEM upon application
1068 of the TRPM3 inhibitor primidone (100 µM) in homozygous (orange) and heterozygous (blue)
1069 transfected HEK293T cells. Cells were transfected with (**A**) TRPM3 wild-type (WT) and non-
1070 transfected cells (NT), and the *TRPM3* variant D614V (**B**), L769V (**C**), V1002M (**D**), V1002G (**E**),
1071 V1002L (**F**), G1007S (**G**), P1102Q (**H**), N1126D (**I**) and S1133P (**J**) (N=3 independent
1072 experiments).
1073
1074 **Figure 3 – Figure Supplement 2**: **PS-induced calcium influxes in TRPM3-DEE mutants.**
1075 Time course of intracellular calcium concentrations, $[Ca^{2+}]_i$ ± SEM upon application of the
1076 pregnenolone sulphate (PS; 40 µM) in homozygous (orange) and heterozygous (blue)
1077 transfected HEK293T cells. Cells were transfected with (**A**) TRPM3 wild-type (WT, black) and
1078 non-transfected cells (NT, grey), the TRPM3 variant D614V (**B**), L769V (**C**), V1002M (**D**),
1079 V1002G (**E**), V1002L (**F**), G1007S (**G**), P1102Q (**H**), N1126D (**I**) and S1133P (**J**) (N=3
1080 independent experiments). For these experiments, the isoform corresponding to GenBank
1081 AJ505026.1 was used.
1082
1083 **Figure 3 – Figure Supplement 3**: **Pregnenolone Sulphate dose dependency of the TRPM3**
1084 **variant G1007S.**
1085 HEK293T cells were transfected with TRPM3 or its mutant G1007S, or a 1:1 ratio of mutant
1086 and wild-type TRPM3 plus the calcium sensor GCaMP6. Fluorescence was measured in a 96-
1087 well plate reader (Flexstation-3). (**A**-**C**) Representative fluorescence traces of wild-type
1088 TRPM3 (**A**), the G1007S mutant (**B**), co-transfection of TRPM3 and G1007S (1:1 ratio) (**C**). The
1089 applications of various concentrations of PS and ionomycin (Iono; 2 µM) are indicated by the
1090 arrows. Basal fluorescence was subtracted and PS-induced Ca^{2+} signals were normalized to
1091 the signal after applying ionomycin. Each single trace shows the average of four replicates

1092 from the same transfection. (**D**) Hill 1 fits of the PS dose dependency of the TRPM3 mutant
1093 G1007S. Symbols represent Mean ± SEM from 3 independent experiments. For these
1094 experiments, the isoform corresponding to NCBI reference sequence NM_001366141.2
1095 cloned in the pcDNA3.1(+)-N-eGFP vector, was used.
1096
1097 **Figure 3 – Figure Supplement 4**: **Fluorescence Intensity of channel-linked YFP in cells**
1098 **expressing WT TRPM3 and TRPM3 variants.**
1099 (**A**) YFP fluorescence in HEK293T cells expressing the indicated variants, with (1:1) or without
1100 co-expression of the WT subunit. Fluorescence values were normalized to the mean YFP
1101 fluorescence of cells expressing WT TRPM3 transfected on the same experimental day. A
1102 one-way ANOVA with Dunnett's posthoc test was used and significant p-values are reported
1103 on the graph. (**B**) Scatter plot (small crosses) of basal $[Ca^{2+}]_i$ levels versus normalized YFP
1104 fluorescence for cells expressing WT TRPM3, D614V and WT+ D614V. The large filled
1105 symbols show the mean basal $[Ca^{2+}]_i$ levels for pooled cells with similar YFP fluorescence.
1106 Cells were binned according to YFP fluorescence with a bin width of 50%. All cells with YFP
1107 levels higher than the highest bin for WT were pooled in the rightmost bin. (**C**) Same as (B),
1108 but for the V1002G variant. Note that the total amount of DNA used for transfection was
1109 identical for all conditions.
1110
1111 **Figure 4 – Figure supplement 1**: **Individual data points of intracellular calcium**
1112 **concentrations at baseline and upon application of the TRPM3 inhibitor primidone.**
1113 Time course of intracellular calcium concentrations, $[Ca^{2+}]_I$ ± SEM upon application of the
1114 pregnenolone sulphate (PS; 40 µM) in homozygous (orange) and heterozygous (blue)
1115 transfected HEK293TIntracellular calcium concentrations ($[Ca2+]_I$), in the absence (Base) and
1116 presence of primidone (Prim; 100 µM). Each individual cells is represented as a single dot
1117 and the same cell is connected with a line before and after the application of primidone. (A)
1118 non-transfected (NT) cells and wild-type (WT) transfected HEK293T cells are represented in
1119 grey and black, respectively. (B-J) Homozygous and heterozygous (WT + mutant construct)
1120 transfected HEK293T cells are represented in orange and blue, respectively. Including the
1121 TRPM3 variant D614V (**B**), L769V (**C**), V1002M (**D**), V1002G (**E**), V1002L (**F**), G1007S (**G**),
1122 P1102Q (**H**), N1126D (**I**) and S1133P (**J**). For these experiments, the isoform corresponding to
1123 GenBank AJ505026.1 was used.

1124

1125 **Figure 4 – Figure supplement 2**: **Individual data points of intracellular calcium amplitudes**
1126 **upon application of the TRPM3 agonist pregnenolone sulphate.**
1127 Corresponding calcium amplitudes ($\Delta[Ca2+]_I$) of the PS responses. Non-transfected (NT) cells
1128 and wild-type (WT) transfected HEK293T cells are represented in grey and black,
1129 respectively. (**A**) Homozygous and (**B**) heterozygous (WT + mutant construct) transfected
1130 HEK293T cells are represented in orange and blue, respectively. Each individual cells is
1131 represented as a single dot and the line represents mean ± SEM. For these experiments, the
1132 isoform corresponding to GenBank AJ505026.1 was used.

1133

1134 **Figure 4 – Figure supplement 3**: **Baseline and PS-induced current densities of the L769V**
1135 **and G1007S substitution.**
1136 (**A**) Representative whole-cell TRPM3 current densities (pA/pF) recorded at baseline without
1137 an agonist (left) and during the application of the agonist pregnenolone sulphate (PS) (right)
1138 during voltage steps ranging from -160 mV to +160 mV, separated by steps of +40 mV for
1139 non-transfected HEK293T cells (NT), wild-type (WT), L769V (LV), WT+ LV, G1007S (GS) and
1140 WT+GS transfected HEK293T cells. (**B-E**) Scatter plot of current densities (pA/pF) for NT, WT,
1141 LV, WT+ LV, GS and WT+GS transfected HEK293T cells (N = 7 for WT and N = 8 for other
1142 conditions) without the application of an agonist at +160 mV (B) and -160 mV (C) and during
1143 the application of PS at +160 mV (D) and -160 mV (E). (**F**) Fraction of current densities
1144 (pA/pF) at baseline compared to current densities when the agonist PS was applied
1145 ($I_{Baseline}/I_{PS}$). Data are represented as mean ± SEM and individual cells are represented as a
1146 dot (B-F). A Kruskal-Wallis ANOVA with Dunn's posthoc test was used. For all plots, relevant
1147 p-values are reported on the graphs and other p-values are reported below. Panel (B) vs NT:
1148 WT ($p > 0.9999$), LV ($p > 0.9999$), WT+LV ($p = 0.0171$), GS ($p = 0.0002$), WT+GS ($p = 0.0056$)
1149 and vs WT: LV ($p > 0.9999$), WT+LV ($p = 0.5596$), WT+GS ($p = 0.2871$); panel (C) vs NT: WT (p
1150 > 0.9999), LV ($p > 0.9999$), WT+LV ($p > 0.9999$), GS ($p > 0.9999$), WT+GS ($p = 0.2326$) and vs
1151 WT: LV ($p > 0.9999$), WT+LV ($p > 0.9999$), GS ($p > 0.9999$), WT+GS ($p > 0.9999$); panel (D) vs
1152 NT: WT ($p = 0.0025$), LV ($p > 0.9999$), WT+LV ($p = 0.0095$), GS ($p = 0.0016$), WT+GS ($p =$
1153 0.0007) and vs WT: WT+LV ($p > 0.9999$), GS ($p > 0.9999$), WT+GS ($p > 0.9999$); panel (E) vs
1154 NT: WT ($p > 0.9999$), LV ($p > 0.9999$), WT+LV ($p = 0.0016$), GS ($p > 0.9999$), WT+GS ($p >$
1155 0.9999) and vs WT: LV ($p = 0.8377$), WT+LV ($p = 0.0993$), GS ($p > 0.9999$), WT+GS ($p >$

1156 0.9999); panel (F) vs NT: WT ($p < 0.0001$), LV ($p > 0.9999$), WT+LV ($p = 0.0010$), GS ($p =$
1157 0.2394), WT+GS ($p = 0.0014$) and vs WT: WT+LV ($p = 0.9001$), WT+GS ($p = 0.7680$). For these
1158 experiments, the isoform corresponding to GenBank AJ505026.1 was used.
1159
1160 **Figure 5 – Figure supplement 1**: **RNA expression of TRPM3 in humans.**
1161 (**A**) RNA-seq tissue data generated by the Genotype-Tissue Expression (GTEx) project,
1162 reported as nTPM (normalized protein-coding transcripts per million), corresponding to
1163 mean values of the different individual samples from each tissue. (**B**) Illustration of human
1164 brain RNA expression levels, where darker color represents higher expression patterns. (**C**)
1165 Illustration of the human brain, where each color represents a different brain region. (**D**)
1166 GTEx Human brain RNA-Seq dataset reported as nTPM. Colors correspond to panel (C).
1167 Figures were adapted from the human protein atlas (proteinatlas.org).
1168
1169 **Figure 5 – Figure supplement 2**: **TRPM3 expression in adult cortex and developing**
1170 **cerebellum.**
1171 (**A**) UMAP visualization of human cortical nuclei annotated on the basis of marker genes. (**B**)
1172 UMAP visualization of human developing cerebellar nuclei annotated on the basis of post
1173 conception weeks (PCW). (**C, D**) The same UMAP visualization of human nuclei as panel (A)
1174 and (B), now representing the expression of TRPM3 for the adult cortex (C) and developing
1175 cerebellum (D), respectively. (**E**) Dot plot showing the expression of one selected marker
1176 gene per cell type for the adult cortex. The size of the dot represents the percentage of
1177 nuclei within a cell type in which that marker was detected and its color represents the
1178 average expression level. Data set of TRPM3 in adult cortex adapted from (32). Data set of
1179 TRPM3 in developing cerebellum adapted from (30).

FIGURE 1

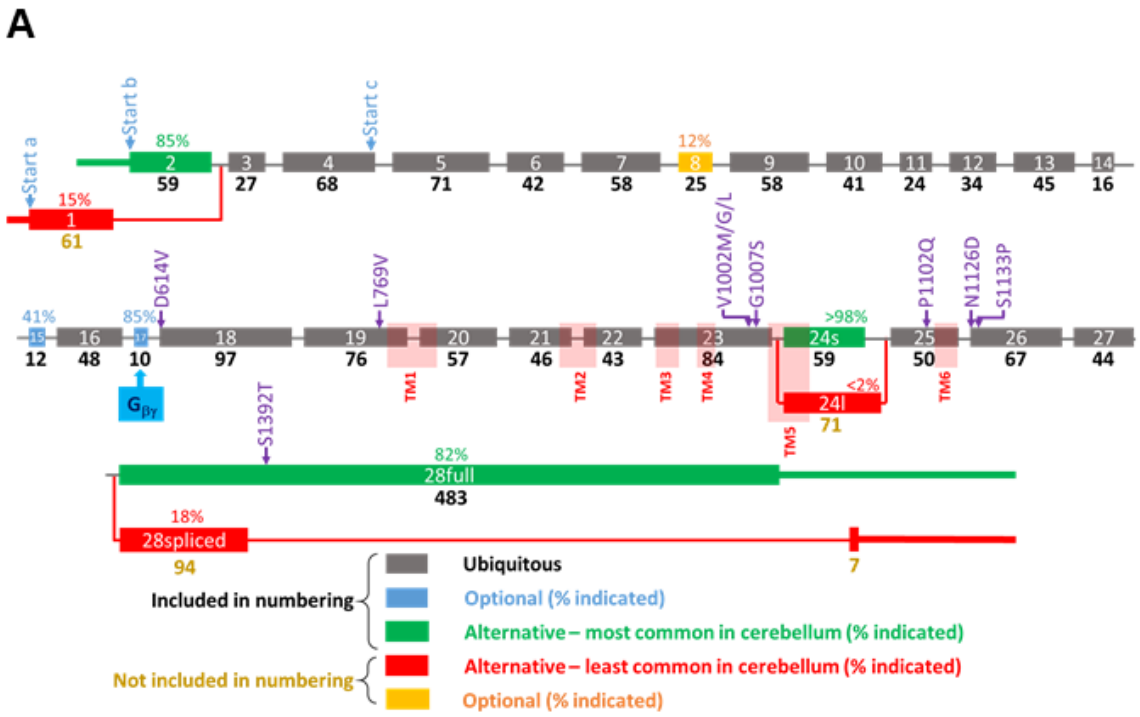
A
Start a
Start b
Start c
85%
15%
12%
2
59
3
27
4
68
5
71
6
42
7
58
8
25
9
58
10
41
11
24
12
34
13
45
14
16
1
61
D614V
L769V
V1002M/G/L
G1007S
P1102Q
N1126D
S1133P
41%
85%
>98%
15
16
17
18
19
20
21
22
23
24s
25
26
27
12
48
10
97
76
57
46
43
84
59
50
67
44
TM1
TM2
TM3
TM4
TM5
TM6
<2%
24l
71
S1392T
82%
28full
483
18%
28spliced
94
7
Included in numbering
Ubiquitous
Optional (% indicated)
Alternative – most common in cerebellum (% indicated)
Not included in numbering
Alternative – least common in cerebellum (% indicated)
Optional (% indicated)
B
D614V
L769V
V1002M/G/L
G1007S
P1102Q
N1126D
S1133P
S1367T
0
100
200
300
400
500
600
700
800
900
1000
1100
1200
1300
1400
1500
1600
1700
1719
28full
TM1
TM2
TM3
TM4
TM5
TM6

FIGURE 1 – FIGURE SUPPLEMENT 1

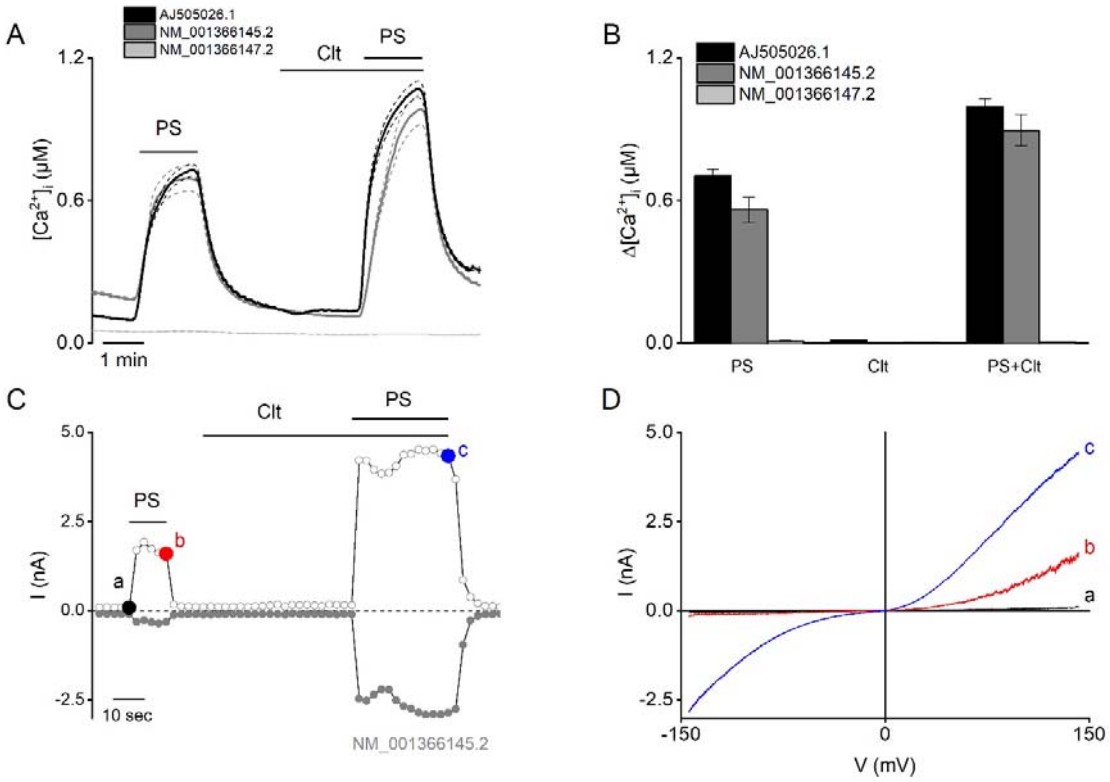

FIGURE 1 – FIGURE SUPPLEMENT 2

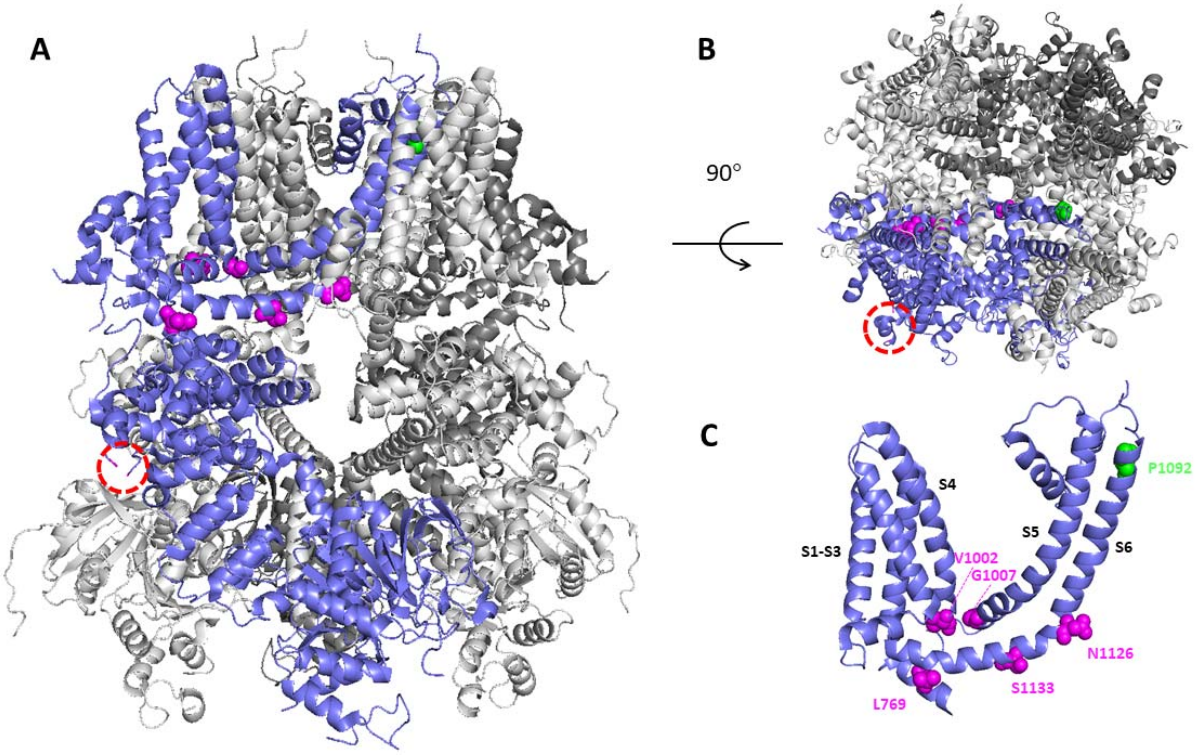

FIGURE 1- FIGURE SUPPLEMENT 3

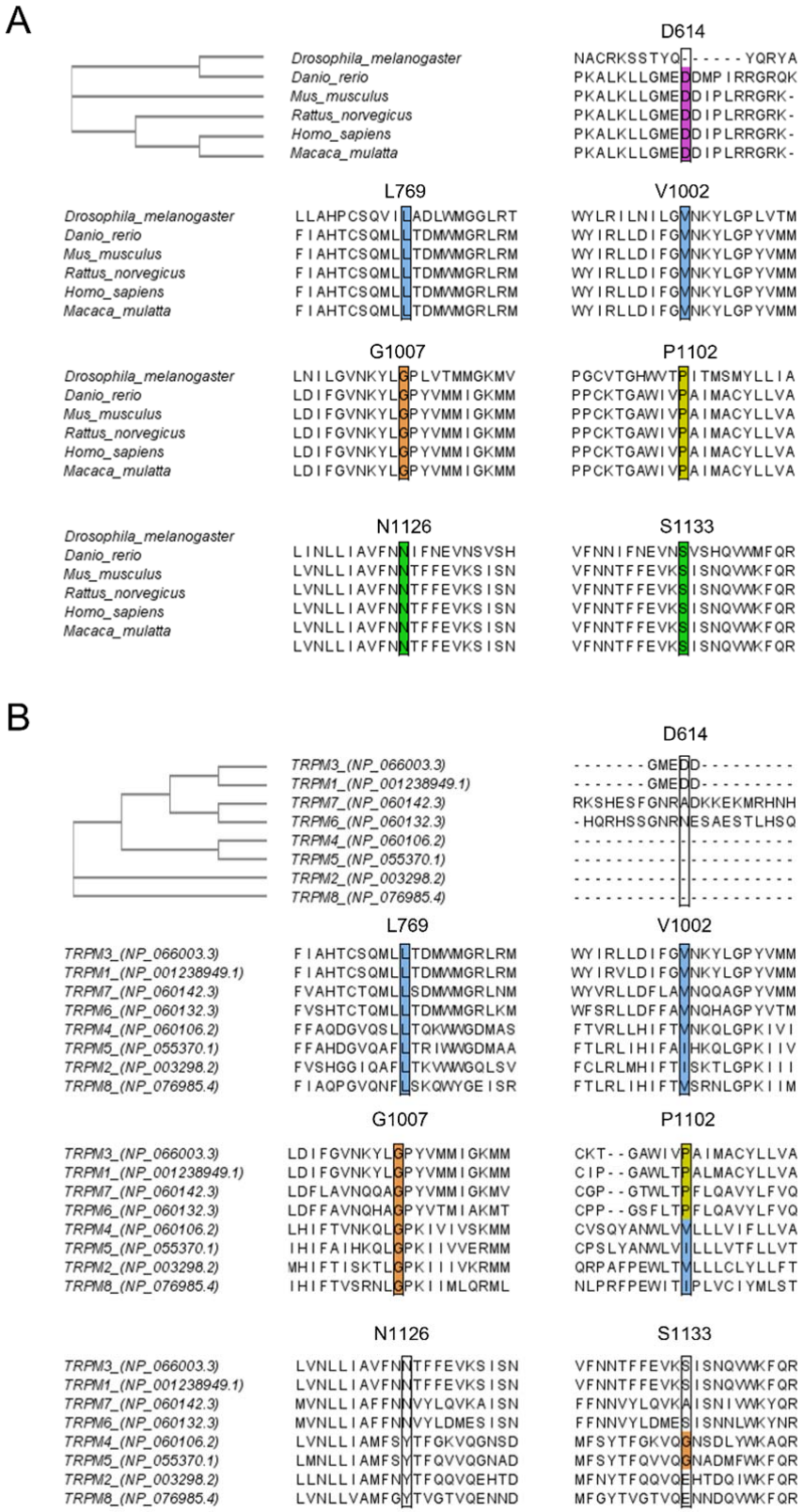

FIGURE 2

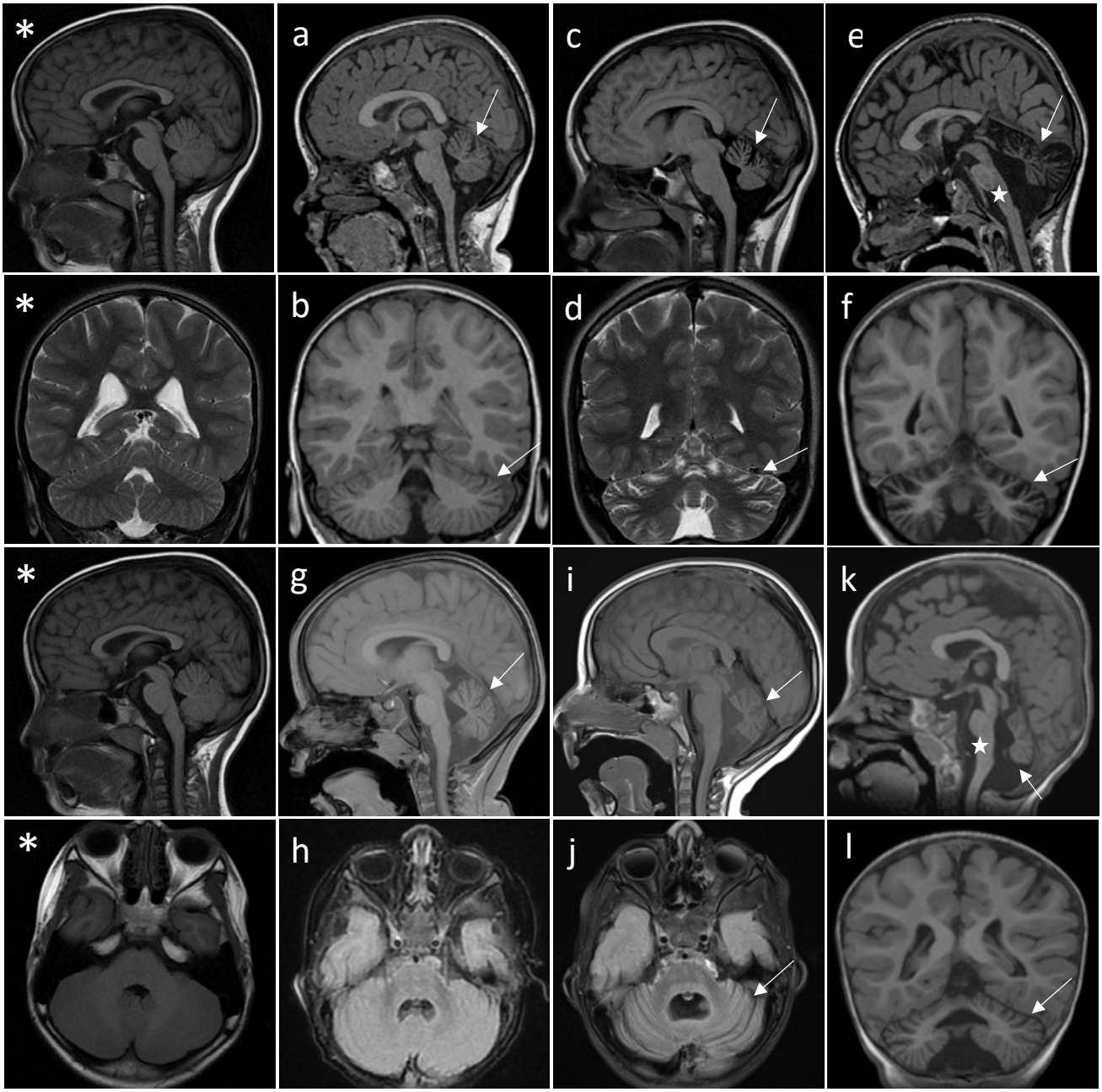

FIGURE 2 – FIGURE SUPPLEMENT 1

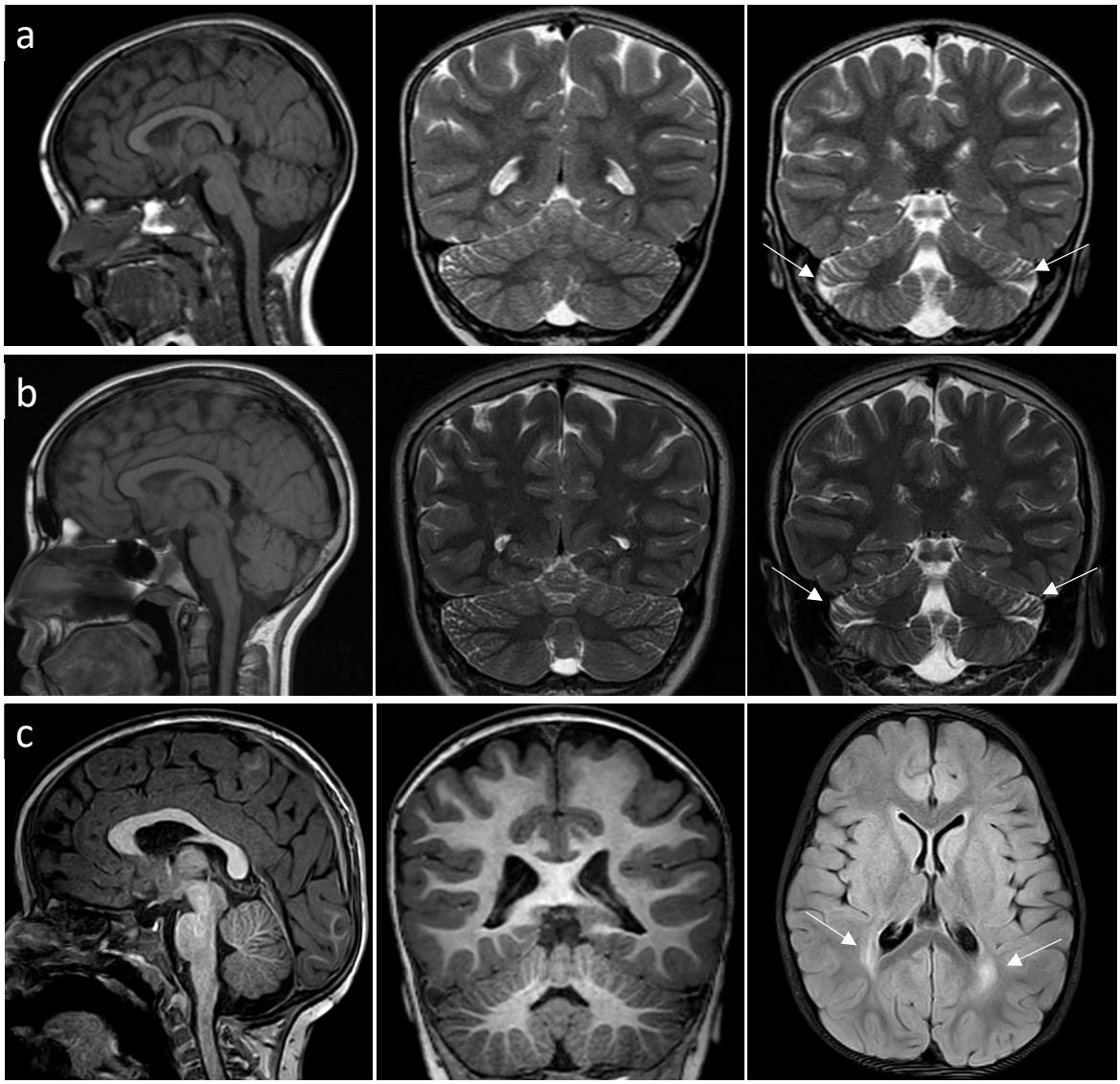

FIGURE 3

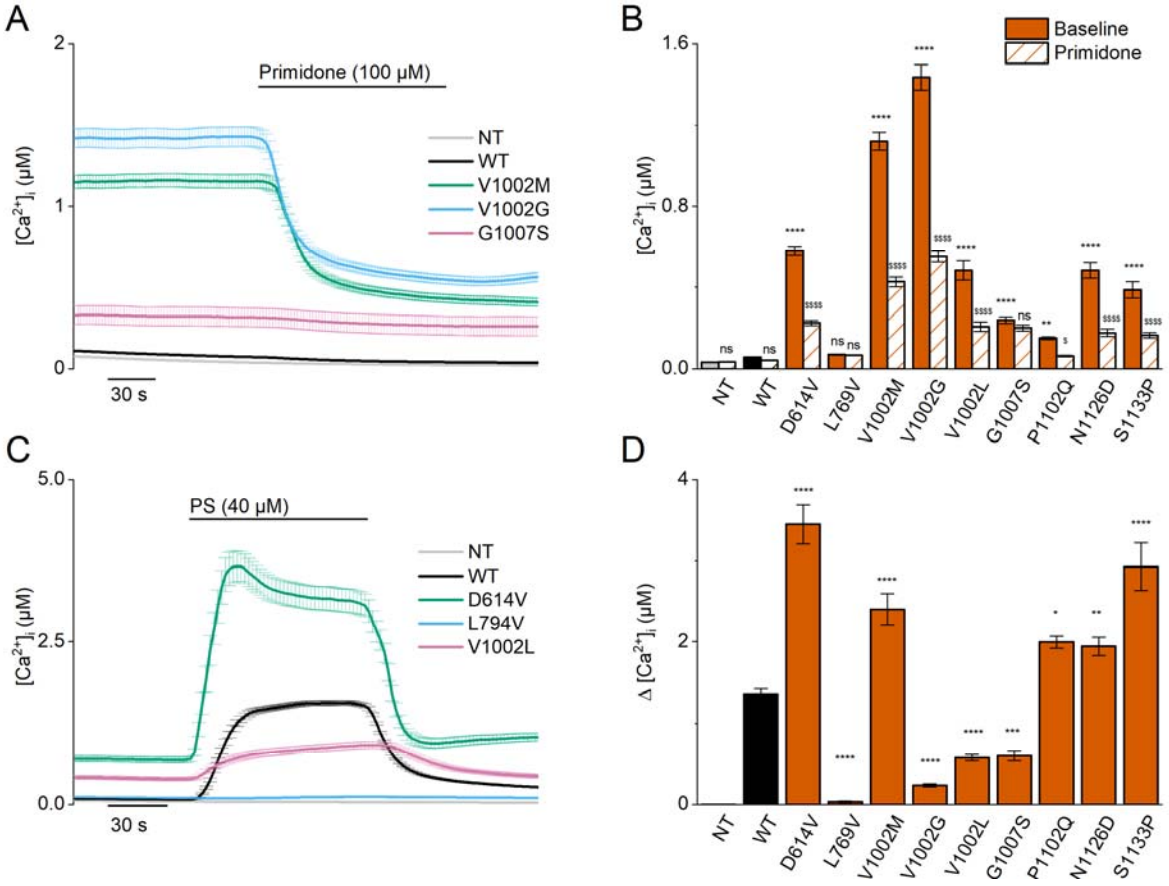
A
Primidone (100 μM)
NT
WT
V1002M
V1002G
G1007S
[Ca2+]i (μM)
30 s
B
Baseline
Primidone
[Ca2+]i (μM)
NT
WT
D614V
L769V
V1002M
V1002G
V1002L
G1007S
P1102Q
N1126D
S1133P
C
PS (40 μM)
NT
WT
D614V
L794V
V1002L
[Ca2+]i (μM)
30 s
D
Δ [Ca2+]i (μM)
NT
WT
D614V
L769V
V1002M
V1002G
V1002L
G1007S
P1102Q
N1126D
S1133P

1 **FIGURE 3 – FIGURE SUPPLEMENT 1**

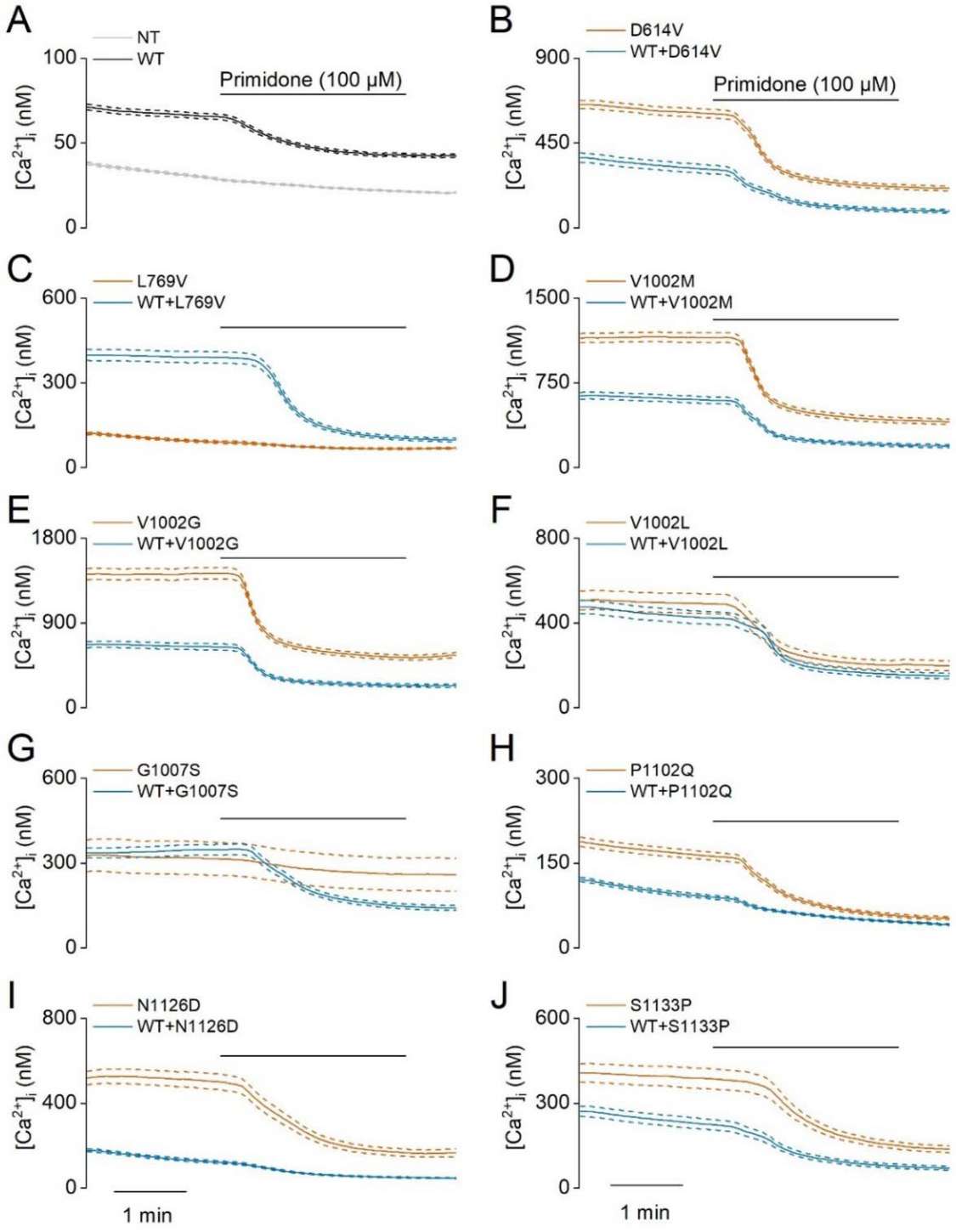

2

FIGURE 3 – FIGURE SUPPLEMENT 2

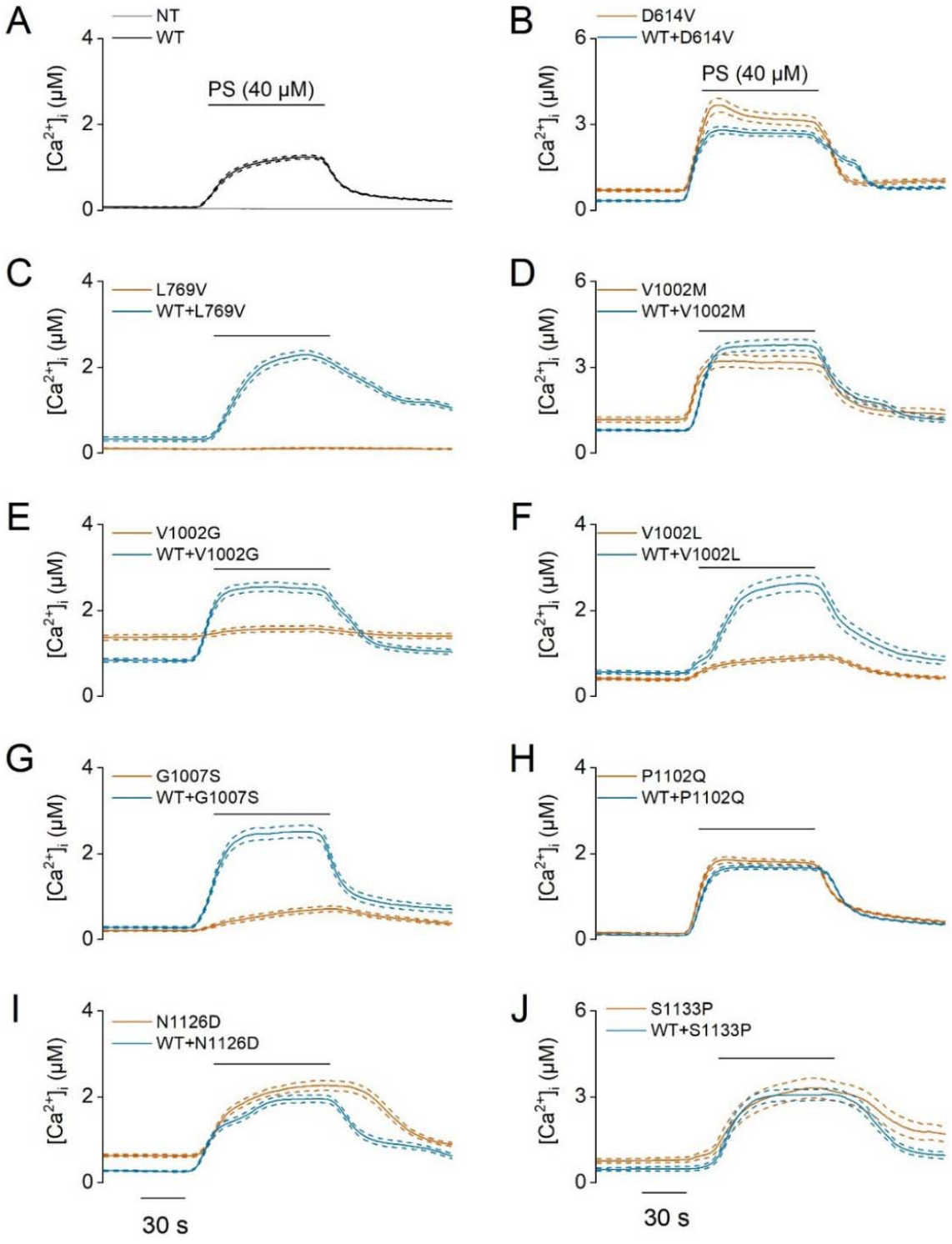

FIGURE 3 – FIGURE SUPPLEMENT 3

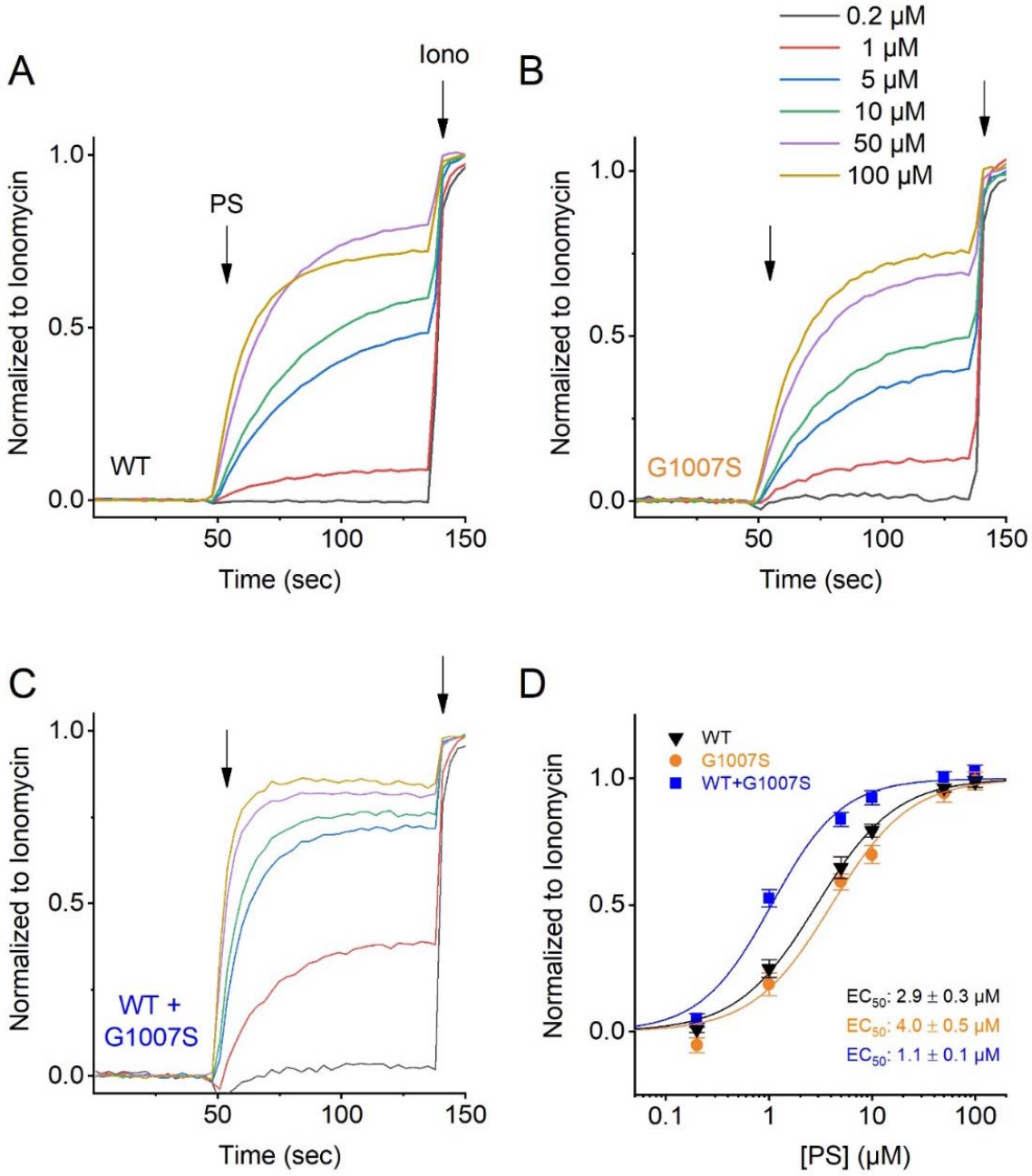

FIGURE 3 – FIGURE SUPPLEMENT 4

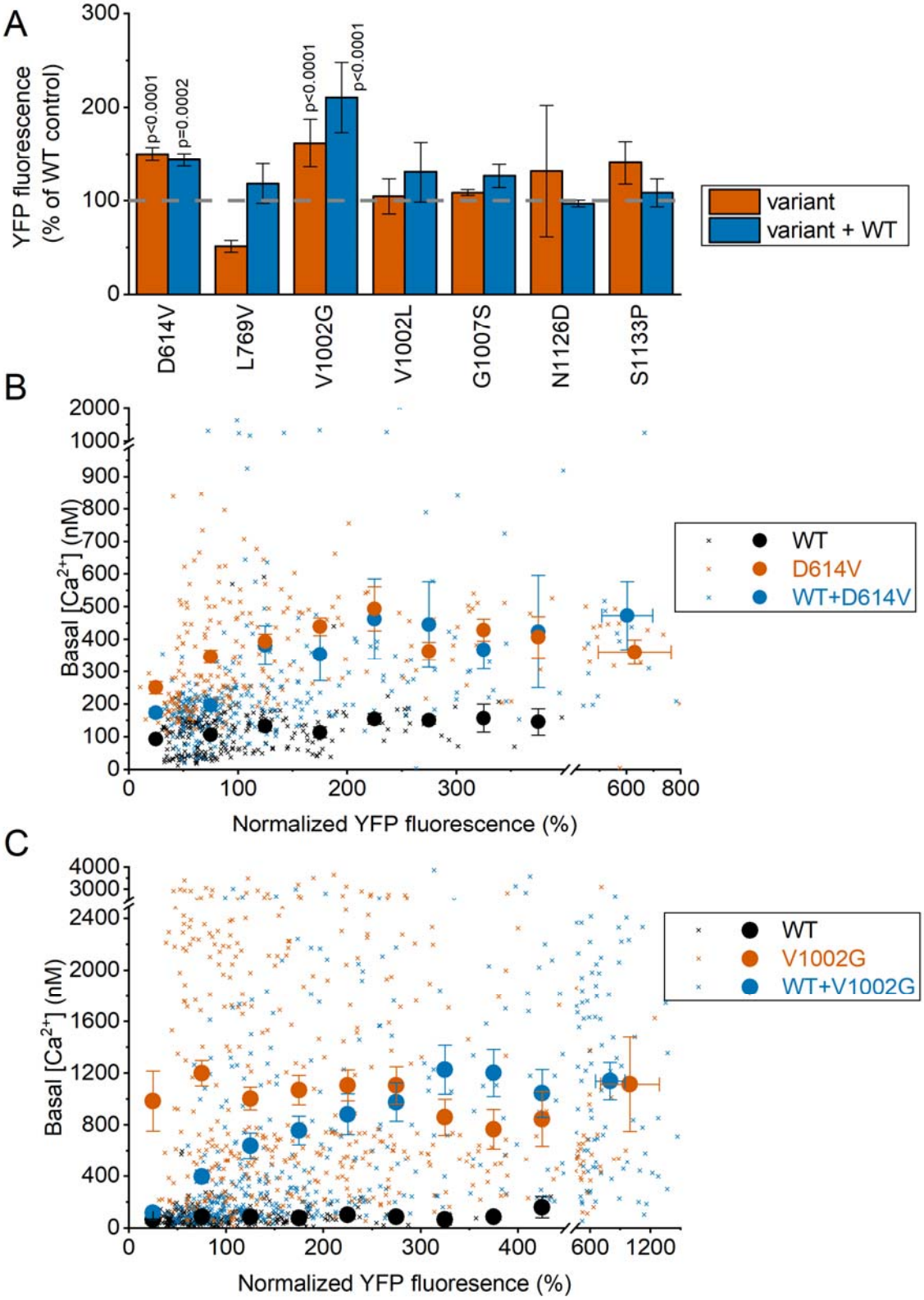

FIGURE 4

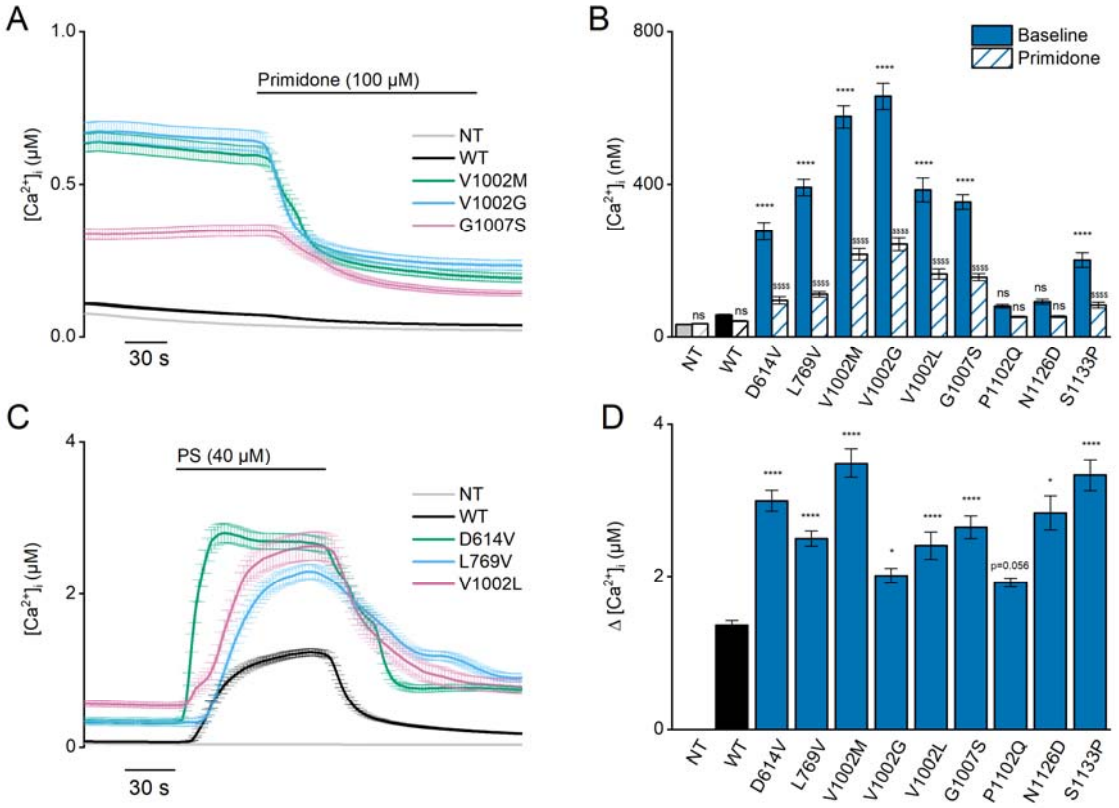
A
Primidone (100 μM)
NT
WT
V1002M
V1002G
G1007S
[Ca2+]i (μM)
30 s
B
Baseline
Primidone
[Ca2+]i (nM)
NT
WT
D614V
L769V
V1002M
V1002G
V1002L
G1007S
P1102Q
N1126D
S1133P
C
PS (40 μM)
NT
WT
D614V
L769V
V1002L
[Ca2+]i (μM)
30 s
D
Δ [Ca2+]i (μM)
p=0.056
NT
WT
D614V
L769V
V1002M
V1002G
V1002L
G1007S
P1102Q
N1126D
S1133P

FIGURE 4 – FIGURE SUPPLEMENT 1

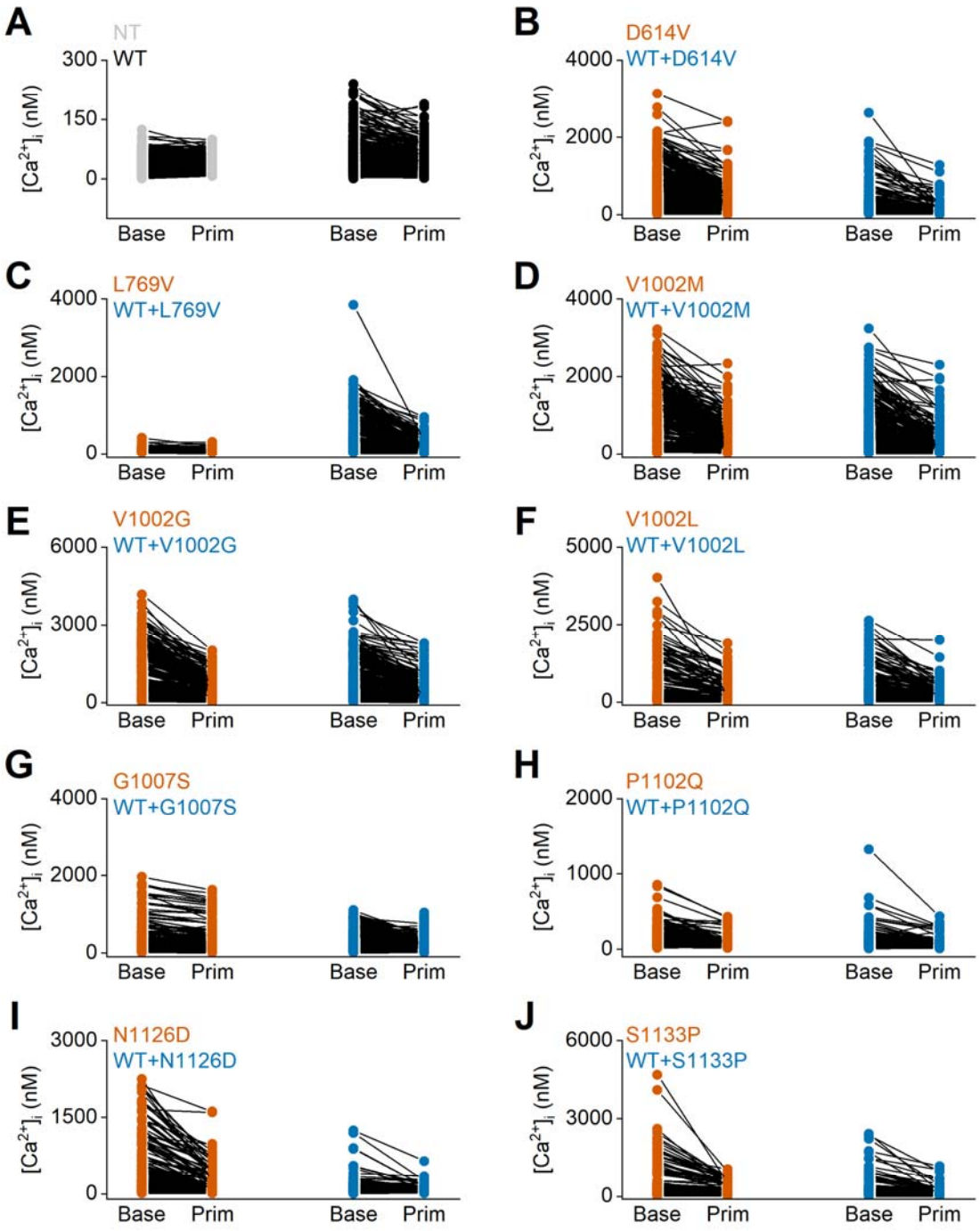

FIGURE 4 – FIGURE SUPPLEMENT 2

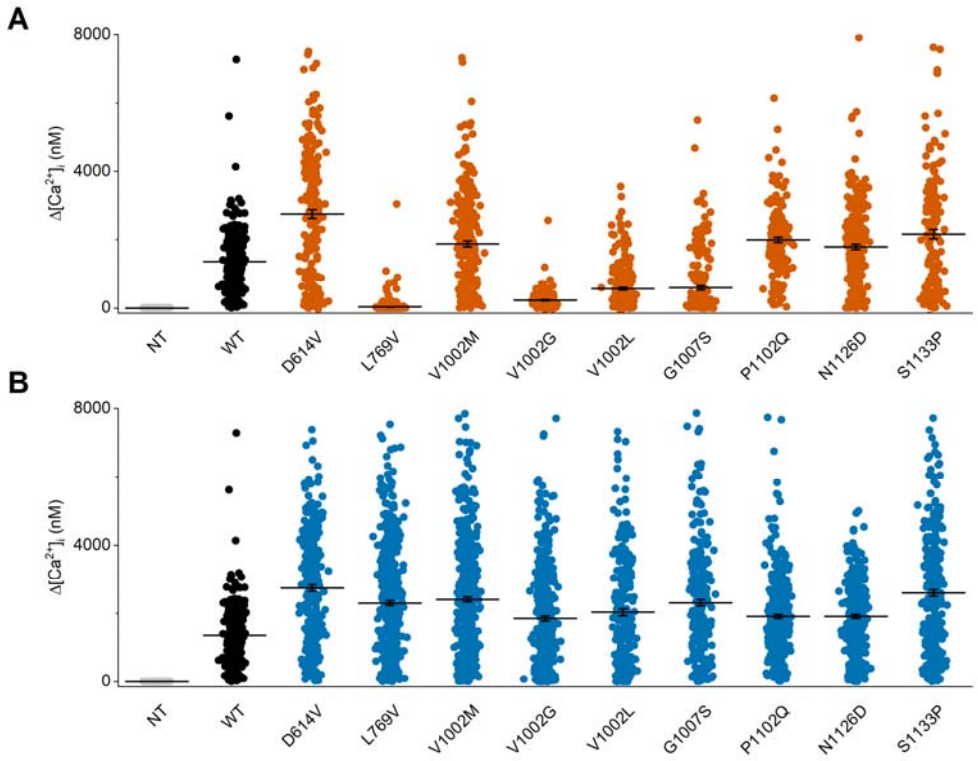

FIGURE 4 – FIGURE SUPPLEMENT 3

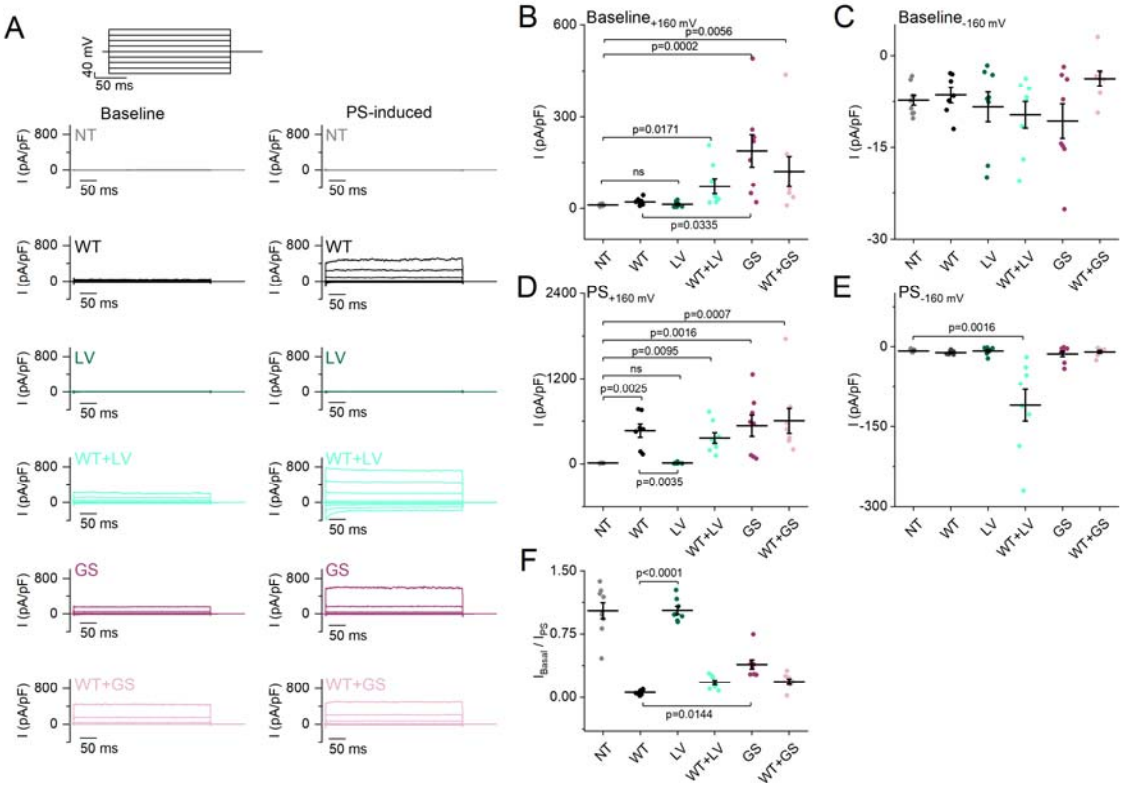

FIGURE 5

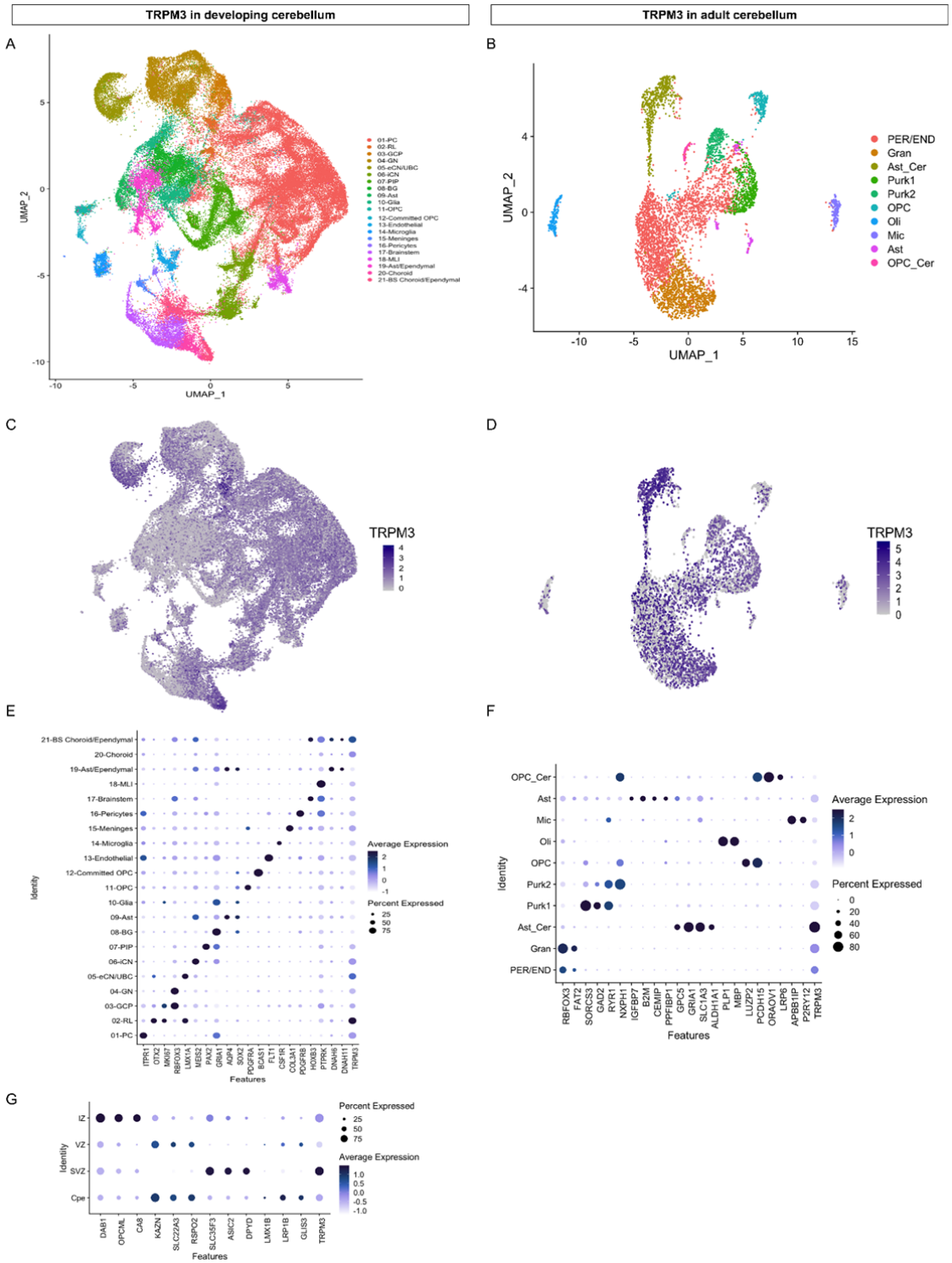
TRPM3 in developing cerebellum
TRPM3 in adult cerebellum
A
B
C
D
E
F
G
UMAP_1
UMAP_2
01-PC
02-RL
03-GCP
04-GN
05-eCN/UBC
06-iCN
07-PIP
08-BG
09-Ast
10-Glia
11-OPC
12-Committed OPC
13-Endothelial
14-Microglia
15-Meninges
16-Pericytes
17-Brainstem
18-MLI
19-Ast/Ependymal
20-Choroid
21-BS Choroid/Ependymal
PER/END
Gran
Ast_Cer
Purk1
Purk2
OPC
Oli
Mic
Ast
OPC_Cer
TRPM3
Average Expression
Percent Expressed
Identity
Features
IZ
VZ
SVZ
Cpe
DAB1
OPCML
CA8
KAZN
SLC22A3
RSPO2
SLC35F3
ASIC2
DPYD
LMX1B
LRP1B
GLIS3
TRPM3

FIGURE 5 – FIGURE SUPPLEMENT 1

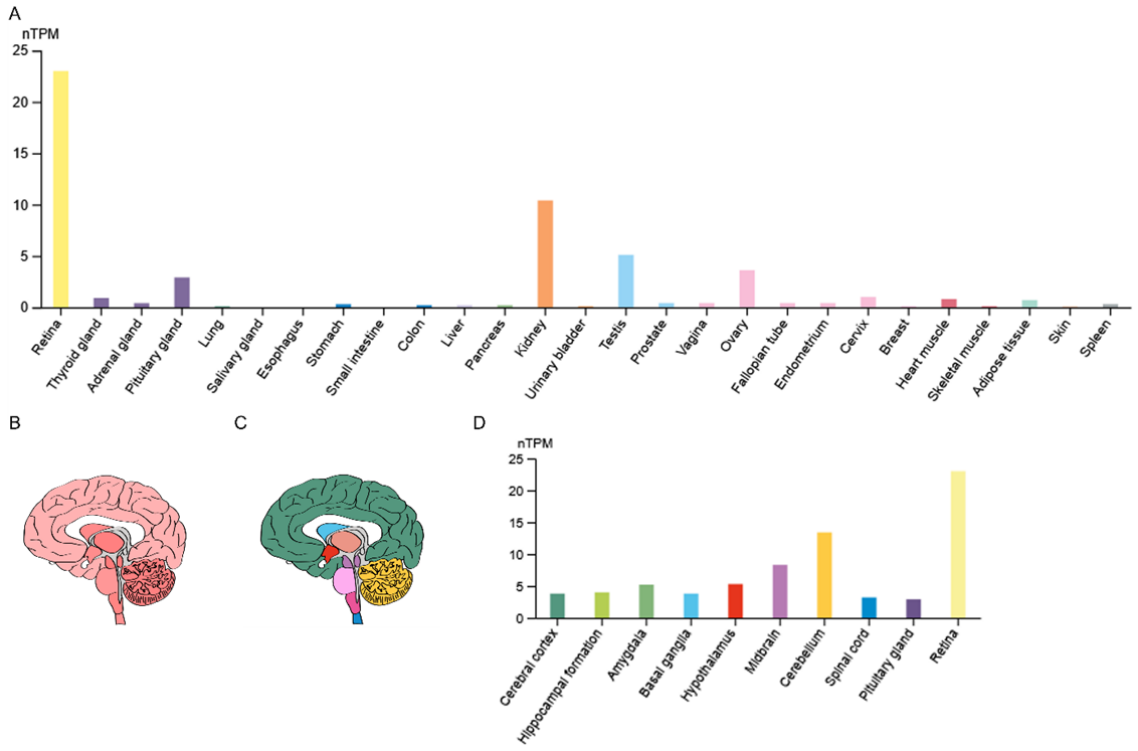

FIGURE 5 – FIGURE SUPPLEMENT 2